A Simple Explanation of Countercyclical Uncertainty[*]

Joshua Bernstein   Michael Plante

Alexander W. Richter   Nathaniel A. Throckmorton

October 10, 2022

ABSTRACT

This paper documents that labor search and matching frictions generate countercyclical uncertainty because the inherent nonlinearity in the flow of new matches makes employment uncertainty increasing in the number of people searching for work. Quantitatively, this mechanism is strong enough to explain uncertainty and real activity dynamics, including their correlation. Through this lens, uncertainty fluctuations are endogenous responses to changes in real activity that neither affect the severity of business cycles nor warrant policy intervention, in contrast with leading theories of the interaction between uncertainty and real activity dynamics.

Keywords: Endogenous Uncertainty; Uncertainty Shocks; Variance Decomposition; Nonlinear
JEL Classifications: C13; D81; E32; E37; J64

1 INTRODUCTION

Countercyclical variation in uncertainty—conditional forecast error volatility of real activity—is a well-documented feature of U.S. data. This paper shows that search and matching frictions embedded in Diamond-Mortensen-Pissarides (DMP) models can explain this empirical fact. Through this lens, uncertainty fluctuations are endogenous responses to the fluctuations in real activity that neither affect the severity of business cycles nor warrant policy intervention. These results highlight the importance of accounting for unemployment dynamics when studying the effect of uncertainty.

Search and matching frictions endogenously generate countercyclical uncertainty because the inherent nonlinearity in the flow of new matches makes employment uncertainty increasing in the number of people searching for work. Intuitively, when the economy is in a recession and more people are looking for work, the flow of new matches becomes more sensitive to changes in the job finding rate. This leads to a wider distribution of new matches and raises employment uncertainty.

We first highlight the key mechanism analytically and then quantify its strength by estimating a nonlinear DMP model with exogenous volatility shocks. The goal of our empirical exercise is to see how far search and matching frictions can take us toward explaining uncertainty dynamics. To identify the model parameters, we target moments of the real uncertainty series in Ludvigson et al. (2021), which captures the common component of uncertainty across 73 real activity measures. This series is useful because it removes the predictable variation in macro aggregates and cleanly maps to business cycle models. We find the model closely matches its standard deviation and negative correlation with output, in addition to a range of typical business cycle moments. Furthermore, the countercyclicality of uncertainty is driven by level shocks, which shows the search and matching mechanism is strong enough to explain the countercyclical uncertainty fluctuations in the data.

We provide additional support for our mechanism through several exercises that show the importance of employment uncertainty in the data. Most notably, we construct an uncertainty series for employment inflows in the data and correlate them with the level of unemployment. We find a strong negative correlation in the data, consistent with the predictions of our DMP model. We also construct an uncertainty series based on the 13 payroll employment series. We find it is strongly correlated with the baseline real uncertainty series and equally countercyclical, providing further support that employment uncertainty plays a key role in the dynamics of the real uncertainty series.

There are two important consequences of our explanation for the countercyclical fluctuations in uncertainty. First, there is minimal feedback from endogenous uncertainty to real activity, a result we confirm by showing the standard deviations of output and unemployment are almost unchanged when we log-linearize our model. Second, countercyclical fluctuations in uncertainty survive when the economy is constrained efficient, so the mere existence of countercyclical uncertainty is not a motive for policy intervention. These results contrast with existing theories of countercyclical un-

certainty that emphasize feedback mechanisms from uncertainty to real activity (e.g., Fajgelbaum et al., 2017) or policy responses to exogenous uncertainty shocks (e.g., Basu and Bundick, 2017).

We also show our results extend to richer models that include Epstein-Zin preferences, nominal price rigidities, downward wage rigidity, convex vacancy costs, endogenous job separations, and variable search intensity. These features have been emphasized in the literature and could affect the strength of the endogenous uncertainty channel. In each case, however, the search and matching mechanism remains strong enough to fully explain the countercyclicality of uncertainty in the data.

Related Literature Petrosky-Nadeau and Zhang (2017) and Petrosky-Nadeau et al. (2018) show that search and matching frictions generate significant skewness and kurtosis in unemployment dynamics. Their results are driven by the concavity in their assumed matching function and the nonlinearity in the flow of new matches. We analytically and numerically show the countercyclicality of uncertainty in our model is entirely driven by the nonlinearity in the flow of new matches.

Our endogenous uncertainty mechanism contributes to existing theories of time-varying endogenous uncertainty. The most relevant papers can be divided into two distinct groups. The first emphasizes that concavity in agents' decision rules endogenously generates countercyclical uncertainty because agents respond more to negative shocks than to positive shocks. For example, Ilut et al. (2018) show that concave hiring rules at the firm level generate a range of nonlinear outcomes including time-varying macroeconomic volatility (i.e., uncertainty).[1] We also focus on the labor market as a source of endogenous uncertainty, but our mechanism works through search and matching frictions rather than agents' decision rules and is robust to the nonlinearities in the hiring rule.

The second group emphasizes the role of information and feedback from uncertainty to real activity. For example, Ilut and Schneider (2014) develop a model in which ambiguity-averse agents receive noisy information about productivity and form expectations using their worst case beliefs. An increase in ambiguity widens their belief set and reduces real activity. Fajgelbaum et al. (2017) present a model in which the level of real activity determines the quality of firms' information about the state of the economy and their investment behavior. Lower activity raises uncertainty, which dampens investment and deepens recessions. Similar mechanisms are at work in Benhabib et al. (2016), Saijo (2017), Straub and Ulbricht (2015) and Van Nieuwerburgh and Veldkamp (2006). Relative to these influential papers, we propose a mechanism that also delivers realistic endogenous uncertainty dynamics, but applies in models with complete information and relies only on typical labor market search and matching frictions. As a result, our model has the appealing property that it explains multiple empirical phenomena while only using the identity for the flow of new matches.

We also contribute to the literature that builds quantitative models with time-varying volatility shocks (Basu and Bundick, 2017; Fernández-Villaverde et al., 2015, 2011; Leduc and Liu, 2016;

---

[1]Straub and Ulbricht (2019) and Atkinson et al. (2022) examine other concave decision rules that create uncertainty.

Mumtaz and Zanetti, 2013). However, our focus on the correlation between uncertainty and output differentiates us from that work, which focus on impulse responses to aggregate uncertainty shocks.

Another important line of research focuses on understanding the relationship between real activity and financial uncertainty (Berger et al., 2020; Bianchi et al., 2018; Caggiano et al., 2021; Caldara et al., 2016). Our work is most closely related to Berger et al. (2020) but differs in two ways. First, our analysis focuses on the uncertainty surrounding real activity, whereas they focus on stock market uncertainty. Second, our work shows how search and matching frictions in the labor market can explain the strong negative correlation between real uncertainty and output, whereas Berger et al. (2020) use skewed productivity shocks to explain their empirical finding that shocks to the VIX index have no impact on output, once one controls for the influence of realized volatility.

Our work also contributes to the discussion about the direction of causality between uncertainty and real activity. Labor search and matching frictions generate strong countercyclical movements in uncertainty with the causality running from real activity to uncertainty. This result is in line with Ludvigson et al. (2021), who use shock-based restrictions that allow the data to speak to this issue. They find strong evidence that real uncertainty responds to unexpected fluctuations in real activity.

To obtain our quantitative results, we make two methodological contributions. First, we show how to use a Total Variance Decomposition in the spirit of Isakin and Ngo (2020) to accurately quantify the contributions of level and volatility shocks to the variances of output and aggregate uncertainty. Our method takes into account nonlinearities and interaction effects, and allows us to decompose total effects into their direct and interaction components. This contrasts with linear Forecast Error Variance Decompositions (FEVDs) that cannot handle nonlinearities, generalized FEVDs (Lanne and Nyberg, 2016) that ignore interaction effects, and the method proposed by Isakin and Ngo (2020) that does not decompose total effects into direct and interaction components.

Second, we combine methods in Atkinson et al. (2022) and Bernstein et al. (2022) and estimate our DMP model using a simulated method of moments that jointly targets real activity, unemployment, and uncertainty moments. This approach yields very precise estimates, particularly for the volatility process that drives exogenous uncertainty. It also builds on existing work such as Justiniano and Primiceri (2008), which only uses time series for real activity in the estimation procedure.

Finally, we note that our analysis focuses on uncertainty at the aggregate level. A separate segment of the literature focus on uncertainty at the micro level (e.g., dispersion in firm-level productivity). Influential papers in this area include Arellano et al. (2019), Bachmann and Bayer (2013), Bloom (2007), Bloom et al. (2018), Christiano et al. (2014), Chugh (2016), Gilchrist et al. (2014), Schaal (2017), and Sedláček (2020). We recognize that firm-level uncertainty shocks may have a larger effect on the business cycle than aggregate uncertainty shocks, as shown in Cesa-Bianchi and Fernandez-Corugedo (2018). Our fundamental point is that search and matching frictions are a powerful source of countercyclical uncertainty that is important to account for in future research.

Outline The paper proceeds as follows. Section 2 introduces our empirical measure of uncertainty. Section 3 lays out our model. Section 4 analytically illustrates the endogenous uncertainty mechanism. Section 5 outlines our quantitative methods. Section 6 describes our main results. Section 7 shows they are robust to adding several popular features our model. Section 8 concludes.

2 MEASURING AGGREGATE UNCERTAINTY

To measure uncertainty, we follow Jurado et al. (2015) and Ludvigson et al. (2021), who define the uncertainty of outcome $y_{j,t}$ as the period-t conditional volatility of its h-period ahead forecast error,

$$\mathcal{U}_{j,t}(h) = \sqrt{E_t[(y_{j,t+h} - E_t[y_{j,t+h}])^2]}.$$

Given a vector of N outcomes $Y_t = [y_{1,t}, y_{2,t}, \ldots, y_{N,t}]'$, aggregate uncertainty is then defined as

$$\mathcal{U}_t(h) = \tfrac{1}{N} \sum_{j=1}^{N} \mathcal{U}_{j,t}(h),$$

which is the cross-sectional average of the individual uncertainty measures. As Jurado et al. (2015) note, this definition has three useful features. First, the conditional volatility calculation removes the predictable variation in each outcome using the conditional expectation, leaving only the variance of the unforecastable component. Second, the aggregation step ensures that this measure captures the common component of uncertainty across a large data set, not idiosyncratic fluctuations in a single time series. Third, this definition of uncertainty cleanly maps to business cycle models.

We focus on the real uncertainty series introduced by Ludvigson et al. (2021).[2] To obtain this measure, they estimate a factor-augmented vector autoregression (FAVAR) with stochastic volatility using monthly data on over 280 macro and financial time series. All series are made stationary and standardized before estimating. The FAVAR produces estimates of $E_t[y_{j,t+h}]$ for each outcome given a forecast horizon, h. The uncertainty of each individual series, $\mathcal{U}_{j,t}(h)$, is constructed using a stochastic volatility model of the forecast errors of each series. The real uncertainty measure is the mean of $\mathcal{U}_{j,t}(h)$ across 73 monthly measures of real activity. Using a quarterly horizon ($h = 3$), we then average across months within each quarter to produce a quarterly real uncertainty series.[3]

Uncertainty Dynamics Figure 1 plots our quarterly real uncertainty series and detrended real GDP from 1963 to 2019. Similar to the monthly series in Jurado et al. (2015) and Ludvigson et al. (2021), the quarterly real uncertainty series is countercyclical, rising during recessions. These patterns are summarized at the top of the figure by several useful statistics that inform our model—the standard deviations of real uncertainty and detrended output, and their correlation. Given the standardization of the data used to construct the real uncertainty series, its standard deviation can be

---

[2]Ludvigson et al. (2021) show that real and financial uncertainty have different causal effects on output in the data.
[3]We obtain a similar uncertainty series if we first aggregate to quarterly data and then estimate the FAVAR model.
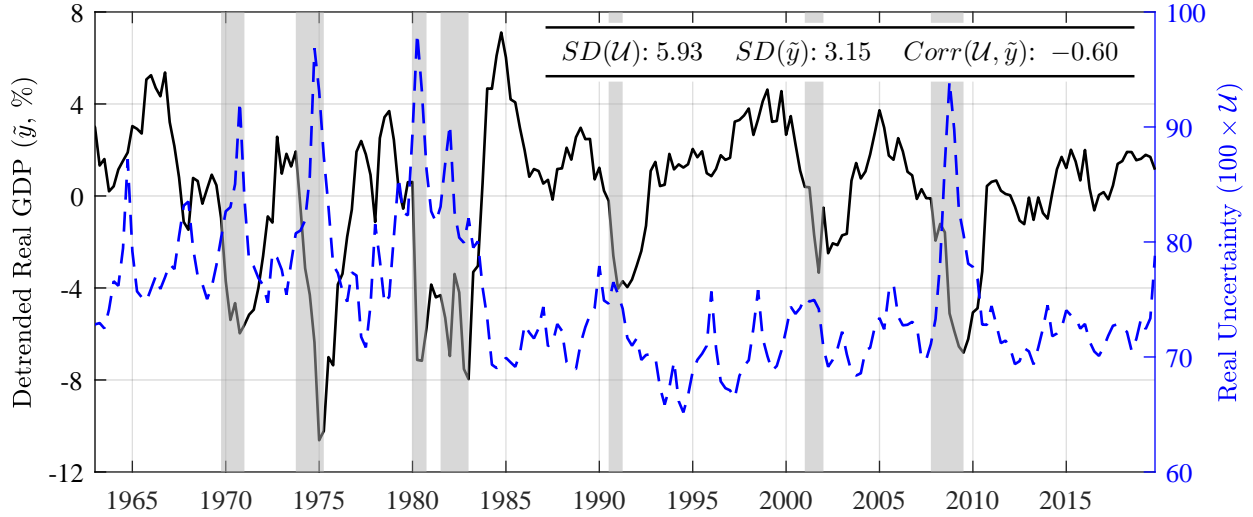
Figure 1: Relationship between output and real uncertainty. Shaded regions denote NBER recessions.

loosely interpreted as 5.93% of the standard deviation of output growth. Therefore, the fluctuations in real uncertainty are considerably smaller than macro aggregates. The countercyclical nature of those fluctuations is captured by the strong -0.60 correlation between real uncertainty and output.[4]

Alternative Uncertainty Measures Our baseline uncertainty measure places equal weight on the 73 underlying uncertainty series. Following Jurado et al. (2015), we also consider the first principal component of the individual uncertainty series. We find this measure has a strong positive correlation with our baseline uncertainty series (0.84) and is slightly more countercyclical (-0.66). While the first principal component loads positively on all 73 uncertainty series, it places higher weight on the uncertainties for several payroll employment and industrial production indicators, suggesting they are important drivers of uncertainty. An uncertainty series based on only the 13 payroll series has a similarly strong correlation with the baseline uncertainty series (0.86) and is strongly countercyclical (-0.56), providing further evidence that uncertainty about employment plays a key role in the behavior of the real uncertainty series and its correlation with real activity.

While there are other uncertainty measures, they are less applicable to our setting. For example, the VIX is often used in financial applications (e.g., Basu and Bundick, 2017; Berger et al., 2020; Bloom, 2009). Over the available sample (1990-2019), this measure is positively correlated with the real uncertainty index (0.56) and negatively correlated with output (-0.37). However, its construction from S&P 500 option prices limits its relevance for our analysis, which is focused on the uncertainty surrounding real activity. Another alternative is to use data on 1-quarter ahead real GDP growth forecasts from the Survey of Professional Forecasters (SPF). For example, tak-

---

[4]These moments are robust to removing the Great Recession period. From 1963-2007, the standard deviations of output and uncertainty were 3.29 and 6.13, respectively, and the correlation between output and uncertainty was -0.57.

ing the inter-quartile range over the available sample (1968-2019) yields a measure of uncertainty that has a strong positive correlation with the real uncertainty series (0.7) and a similar correlation with output (-0.5). However, this measure is likely contaminated by idiosyncratic noise due to the heterogeneous and incomplete information sets of the individual forecasters in the survey. In contrast, the real uncertainty index is constructed using a single information set that is as complete as possible. This aligns well with our model that assumes agents have a complete information set.[5]

3 THEORETICAL MODEL

We use a textbook DMP model that is augmented to include risk-averse households, a capital stock, and investment adjustment costs. Each period corresponds to one month. A representative household owns the capital stock and chooses investment subject to capital adjustment costs. It chooses consumption by pooling the incomes of employed and unemployed workers, ensuring perfect consumption insurance (Andolfatto, 1996; Den Haan et al., 2000; Merz, 1995). A representative firm rents capital in a competitive market and posts vacancies subject to search and matching frictions. As our analytics will show, none of the extra features are necessary to endogenously generate countercyclical uncertainty. We include them for our quantitative analysis, which examines the strength of the search and matching mechanism, subject to matching a battery of business cycle moments.

Business cycle dynamics are driven by shocks to technology (TFP). The level of TFP follows

$$\ln a_t = (1 - \rho_a) \ln \bar{a} + \rho_a \ln a_{t-1} + \sigma_{a,t-1} \varepsilon_{a,t}, \quad -1 < \rho_a < 1, \ \varepsilon_{a,t} \sim \mathbb{N}(0,1). \tag{1}$$

The second driving force determines the volatility of TFP, which follows an independent process

$$\ln \sigma_{a,t} = (1 - \rho_{sv}) \ln \bar{\sigma}_a + \rho_{sv} \ln \sigma_{a,t-1} + \sigma_{sv} \varepsilon_{sv,t}, \quad -1 < \rho_{sv} < 1, \ \varepsilon_{sv,t} \sim \mathbb{N}(0,1). \tag{2}$$

Therefore, TFP is subject to volatility shocks, $\varepsilon_{sv,t}$, that exogenously determine the time-variation in the standard deviation, $\sigma_{a,t}$, of first moment shocks, $\varepsilon_{a,t}$. Following Berger et al. (2020), we lag σ_a in (1) to separate out current volatility from expected future volatility. However, we found that the timing has very little effect on our quantitative results. Specifying TFP in logs ensures that we do not introduce exogenous curvature into the log production function, which will be linear in $\ln a_t$.

Search and Matching Entering period t, there are n_{t-1} employed workers and $u_{t-1} = 1 - n_{t-1}$ unemployed workers. A fraction $\bar{s}$ of employed workers then exogenously lose their jobs. Given that each period corresponds to one month, a fraction $\chi \in [0,1]$ of newly separated workers start searching for jobs in period t. Therefore, the mass of unemployed searching workers in period t is

$$u_t^s = u_{t-1} + \chi \bar{s} n_{t-1}. \tag{3}$$

---

[5]Fajgelbaum et al. (2017) develop a model of uncertainty driven by limited information and thus map to the SPF.

If the firm posts v_t vacancies, the matching process is described by the Cobb-Douglas function,

$$\mathcal{M}(u_t^s, v_t) = \xi(u_t^s)^\phi v_t^{1-\phi}, \tag{4}$$

$$m_t = \min\{\mathcal{M}(u_t^s, v_t), u_t^s, v_t\}, \tag{5}$$

where $\xi > 0$ is matching efficiency and $\phi \in (0, 1)$ is the elasticity of matches with respect to unemployed searching. The employment law of motion, job finding rate, and job filling rate are given by

$$n_t = (1 - \bar{s})n_{t-1} + m_t, \tag{6}$$

$$f_t = m_t/u_t^s, \tag{7}$$

$$q_t = m_t/v_t. \tag{8}$$

Households The representative household pools the income of its employed and unemployed members to achieve perfect consumption insurance. It also chooses investment subject to a capital adjustment cost. With the specification in Jermann (1998), the law of motion for capital is given by

$$k_t = (1 - \delta)k_{t-1} + \left(a_1 + \frac{a_2}{1 - 1/\nu}\left(\frac{i_t}{k_{t-1}}\right)^{1-1/\nu}\right)k_{t-1}, \tag{9}$$

where $0 < \delta \leq 1$ is the capital depreciation rate, $\nu > 0$ determines the size of the capital adjustment cost, and $a_1 = \delta/(1 - \nu)$ and $a_2 = \delta^{1/\nu}$ are chosen so there are no adjustment costs in steady state.

The household chooses consumption, investment, and capital to solve

$$J_t^H = \max_{c_t, i_t, k_t} \ln c_t + \beta E_t[J_{t+1}^H]$$

subject to (9) and

$$c_t + i_t = w_t n_t + r_t^k k_{t-1} + bu_t - \tau_t + d_t,$$

where w_t is the wage rate, r_t^k is the rental rate of capital, b is the flow value of unemployment, τ_t is a lump-sum tax, and d_t are lump-sum dividends from firm ownership. Letting $x_{t+1} = \beta(c_t/c_{t+1})$ denote the household's pricing kernel, the optimality conditions for capital and investment imply

$$\frac{1}{a_2}\left(\frac{i_t}{k_{t-1}}\right)^{1/\nu} = E_t\left[x_{t+1}\left(r_{t+1}^k + \frac{1}{a_2}\left(\frac{i_{t+1}}{k_t}\right)^{1/\nu}(1 - \delta + a_1) + \frac{1}{\nu - 1}\frac{i_{t+1}}{k_t}\right)\right]. \tag{10}$$

Firms The representative firm combines capital and labor to produce the final good with a Cobb-Douglas production function, $y_t = a_t k_{t-1}^\alpha n_t^{1-\alpha}$. It posts vacancies at cost κ to attract new workers, so $d_t = y_t - w_t n_t - r_t^k k_{t-1} - \kappa v_t$. The firm chooses capital, employment, and vacancies to solve

$$J_t^F = \max_{k_{t-1}, n_t, v_t} d_t + E_t[x_{t+1} J_{t+1}^F]$$

7

subject to

$$n_t = (1 - \bar{s})n_{t-1} + q_t v_t,$$

$$v_t \geq 0.$$

Letting $\lambda_{n,t}$ denote the Lagrange multiplier on the law of motion for employment and $\lambda_{v,t}$ denote the multiplier on the non-negativity constraint for vacancies, the optimality conditions are given by

$$r_t^k = \alpha y_t / k_{t-1}, \tag{11}$$

$$\lambda_{n,t} = (1 - \alpha)y_t / n_t - w_t + (1 - \bar{s})E_t[x_{t+1}\lambda_{n,t+1}], \tag{12}$$

$$q_t \lambda_{n,t} = \kappa - \lambda_{v,t}, \tag{13}$$

$$\lambda_{v,t} v_t = 0, \quad \lambda_{v,t} \geq 0. \tag{14}$$

Wages We follow the bulk of the literature and assume wages are determined via Nash bargaining between employed workers and the firm. Let $\eta \in [0, 1]$ denote a worker's bargaining weight and define $\theta_t = v_t / u_t^s$ as labor market tightness. Using the steps in Appendix A, the wage rate satisfies

$$w_t = \eta((1 - \alpha)y_t / n_t + \kappa(1 - \chi\bar{s})E_t[x_{t+1}\theta_{t+1}]) + (1 - \eta)b. \tag{15}$$

Equilibrium Given d_t and $\tau_t = bu_t$, the aggregate resource constraint is given by

$$c_t + i_t + \kappa v_t = a_t k_{t-1}^\alpha n_t^{1-\alpha}. \tag{16}$$

The equilibrium consists of infinite sequences of quantities $\{k_t, c_t, n_t, i_t, u_t^s, v_t, m_t, \mathcal{M}_t, q_t, f_t\}_{t=0}^\infty$, prices $\{w_t, r_t^k, \lambda_{n,t}, \lambda_{v,t}\}_{t=0}^\infty$, and exogenous variables $\{a_t, \sigma_{a,t}\}_{t=0}^\infty$ that satisfy (1)-(16), given an initial state of the economy $\{k_{-1}, n_{-1}, a_{-1}, \sigma_{a,-1}\}$ and the sequences of TFP shocks $\{\varepsilon_{a,t}, \varepsilon_{sv,t}\}_{t=0}^\infty$.

Uncertainty As noted in Section 2, our empirical measure of real uncertainty captures the common component of uncertainty across 73 standardized measures of real activity, which is important for removing the influence of idiosyncratic noise in a particular uncertainty series. In our model, the uncertainties of all variables are driven by common components that exhibit similar volatilities and strong positive correlations. Thus, we follow Plante et al. (2018) and Atkinson et al. (2022) and define aggregate uncertainty in the model as the uncertainty of output growth at a quarterly horizon,

$$\mathcal{U}_t = \tfrac{1}{SD(\Delta y)} \sqrt{E_t[(\ln(y_{t+3}/y_t) - E_t[\ln(y_{t+3}/y_t)])^2]}. \tag{17}$$

This definition is equivalent to the uncertainty surrounding the *level* of log output over a quarterly horizon because y_t is known at time t and cancels from the definition of uncertainty in (17). We normalize in (17) by the standard deviation of output growth in the ergodic distribution, $SD(\Delta y)$, so the units are consistent with our empirical uncertainty measure based on standardized time series.

4 ENDOGENOUS UNCERTAINTY MECHANISM

This section analytically shows that search and matching frictions endogenously generate countercyclical fluctuations in employment uncertainty. Output uncertainty inherits the fluctuations in employment uncertainty via the production function. The derivations are provided in Appendix B.

To begin our analysis, consider a variant of the law of motion for employment given by

$$\hat{n}_{t+1} \equiv n_{t+1}/n_t = 1 - \bar{s} + m_{t+1}/n_t.$$

We can express the flow of new matches as $m_{t+1} = f_{t+1} u_{t+1}^s$, where the stock of people searching for work, $u_{t+1}^s = u_t + \chi \bar{s} n_t$, is pre-determined. Then employment growth uncertainty is given by[6]

$$\sqrt{V_t[\hat{n}_{t+1}]} = \frac{1}{n_t} u_{t+1}^s \sqrt{V_t[f_{t+1}]}.$$

A solution for the job finding rate, f_{t+1}, exists under some assumptions. Following Bernstein et al. (2022), assume vacancies are positive ($\lambda_{n,t} = 0$), labor is the only input in production ($\alpha = 0$), households are risk neutral (linear utility), the wage rate is fixed ($\eta = 0$), and the TFP process is specified in levels instead of logs. We can then guess and verify the solution for the match value is

$$\lambda_{n,t} = \delta_0 + \delta_1(a_t - \bar{a}),$$

where

$$\delta_0 = \frac{\bar{a} - b}{1 - \beta(1 - \bar{s})} > 0, \qquad \delta_1 = \frac{1}{1 - \beta(1 - \bar{s})\rho_a} > 0.$$

Given the solution for $\lambda_{n,t}$, $f_t = \xi^{1/\phi}(\lambda_{n,t}/\kappa)^{(1-\phi)/\phi}$. This shows $V_t[f_{t+1}] \propto V_t[\lambda_{n,t+1}^{(1-\phi)/\phi}]$. Imposing the typical assumption that $\phi = 0.5$, leads to a closed-form expression for employment uncertainty.

Proposition 1. *Consider a labor search and matching model where households are risk neutral, labor is the only input in production, the wage rate is fixed, and TFP follows a level linear process with stochastic volatility. If the matching elasticity, $\phi = 0.5$, then employment uncertainty follows*

$$\sqrt{V_t[\hat{n}_{t+1}]} = \frac{1}{n_t} u_{t+1}^s (\delta_1 \xi^2/\kappa) \sigma_{a,t},$$

which endogenously varies due to changes in u_{t+1}^s and exogenously varies due to changes in $\sigma_{a,t}$.

This result shows that employment uncertainty is increasing in unemployment and therefore endogenously countercyclical. This is due to the inherent nonlinearity in the labor market flow identity, $m_{t+1} = f_{t+1} u_{t+1}^s$, which is commonly used in empirical work (e.g., Shimer, 2005) and appears in any model with search and matching frictions. Intuitively, when the economy is in a

---

[6]Up to a first-order approximation, $\Delta \ln \hat{n}_{t+1} = \hat{n}_{t+1} - 1$, so $V_t[\Delta \ln \hat{n}_{t+1}] = V_t[\ln \hat{n}_{t+1}] \approx V_t[\hat{n}_{t+1}]$. Thus, uncertainty about a gross change in a variable is approximately equal to uncertainty about a log level and log growth rate.

recession and more people are looking for work, the flow of new matches becomes more sensitive to changes in the job finding rate. This leads to a wider distribution of new matches and raises employment uncertainty. The matching function itself plays no role in generating countercyclical uncertainty for two reasons. First, the job finding rate is linear in the match value, $\lambda_{n,t}$. Second, the match value only depends on the exogenous TFP state, a_t. Section 6 shows the matching function also plays no role in our estimated DMP model that relaxes all of the assumptions in Proposition 1.

5 QUANTITATIVE METHODS

This section describes how we quantify the importance of endogenous uncertainty. We first explain how we solve and estimate our model, including how each parameter is identified. We then show how we decompose the variances of output and uncertainty. Appendix C provides our data sources.

5.1 SOLUTION METHOD   We solve the nonlinear model globally using the policy function iteration algorithm described in Richter et al. (2014), which is based on the theoretical work in Coleman (1991). The algorithm minimizes the Euler equation errors on each node in the state space and computes the maximum change in the policy functions. It then iterates until the maximum change is below a specified tolerance criterion. Appendix D describes the solution method in more detail.

5.2 ESTIMATION ALGORITHM   Five parameters are set externally. The time discount factor, β, is set to 0.9983, which implies an annual real interest rate of 2%. The capital depreciation rate, $\delta = 0.0079$, matches the annual average rate on private fixed assets and durable goods converted to a monthly rate. The income share of capital, $\alpha = 0.3888$, equals the complement of the quarterly labor share in the non-farm business sector. The steady-state job separation rate, $\bar{s}$, is set to 0.0328 to match its sample mean. Finally, the steady-state job filling rate is set to 0.3306. This corresponds to a quarterly filling rate of 0.7, which matches Den Haan et al. (2000) and Leduc and Liu (2016).

The remaining parameters are estimated with the Simulated Method of Moments (SMM) procedure used in Atkinson et al. (2022). The algorithm has two steps. First, we estimate the empirical targets with a two-step Generalized Method of Moments (GMM) procedure. The estimates are stored in $\hat{\Psi}_T^D$. Second, we find the parameters that minimize the distance between the empirical targets and equivalent moments from the nonlinear DMP model. To compute the model-implied moments, we simulate the nonlinear DMP model $R = 1{,}000$ times, where each simulation is based on a different sequence of random shocks that lasts for $T = 687$ months to match the length of our data sample. The model analogues of the empirical targets are the mean moments across the R simulations, $\bar{\Psi}_{R,T}^M(\mathcal{P}, \mathcal{E})$, where $\mathcal{P}$ is a vector of parameters and $\mathcal{E}$ is a $T \times 2$ matrix of level and volatility shocks to TFP. The parameter estimates, $\hat{\mathcal{P}}$, are obtained by minimizing the following function:

$$J(\mathcal{P}, \mathcal{E}) = [\hat{\Psi}_T^D - \bar{\Psi}_{R,T}^M(\mathcal{P}, \mathcal{E})]'[\hat{\Sigma}_T^D(1 + 1/R)]^{-1}[\hat{\Psi}_T^D - \bar{\Psi}_{R,T}^M(\mathcal{P}, \mathcal{E})],$$

where $\hat{\Sigma}_T^D$ is the diagonal of the GMM estimate of the variance-covariance matrix for the targets.

We use a bootstrap procedure to calculate standard errors on the parameter estimates.[7] Specifically, we run our SMM algorithm $N_s = 200$ times, each time drawing the shocks using a different seed, s, but leaving $\hat{\Psi}_T^D$ and $\hat{\Sigma}_T^D$ unchanged. Given the set of parameter estimates $\{\hat{\mathcal{P}}^s\}_{s=1}^{N_s}$, we report the mean, $\bar{\mathcal{P}} = \sum_{s=1}^{N_s} \hat{\mathcal{P}}^s / N_s$, and standard errors. This method is numerically intensive but has two major benefits. First, it provides more reliable estimates of the standard errors than the asymptotic variance of the estimator. Second, it is an effective way to determine whether the parameters are identified and check for multiple modes. Appendix E provides further information.

The targets are based on quarterly data in percent deviations from a Hamilton (2018) filtered trend.[8] Each period in the model is 1 month, so we aggregate the simulated data to a quarterly frequency. We then detrend the simulated data by computing log deviations from the time average, so the units of the moments are directly comparable to their empirical counterpart. We compute uncertainty over a 3-month horizon ($h = 3$) in order to match the horizon of the real uncertainty series.

5.3 IDENTIFICATION   We estimate $\mathcal{P} = (b, \phi, \eta, \kappa, \chi, \nu, \rho_a, \bar{\sigma}_a, \rho_{sv}, \sigma_{sv})'$. While each parameter is jointly estimated, we can heuristically describe how each one is identified based on specific moments in the data. Table 1 summarizes the identification scheme, which builds on the methods in Atkinson et al. (2022) and Bernstein et al. (2022). For simplicity, we explain our identification scheme using steady-state conditions, but the intuition applies to the dynamic equilibrium system.

Parameters	Identifying Moments	Parameters	Identifying Moments
b, ϕ	$SD(\tilde{u}), SD(\tilde{v})$	ν	$SD(\tilde{c}), SD(\tilde{\imath}), AC(\tilde{c}), AC(\tilde{\imath})$
η	$Cov(\tilde{w}, \tilde{\ell})/V(\tilde{\ell})$	$\rho_a, \bar{\sigma}_a$	$AC(\tilde{y}), SD(\tilde{y})$
κ, χ	$E(u), E(f)$	ρ_{sv}, σ_{sv}	$AC(\mathcal{U}), SD(\mathcal{U}), Corr(\mathcal{U}, \tilde{y})$

Table 1: Identification heuristic. E, SD, V, AC, $Corr$, and Cov denote the average, standard deviation, variance, autocorrelation, cross-correlation, and covariance over time. A tilde denotes a detrended variable.

The outside option b governs the economy's "fundamental surplus fraction" (Ljungqvist and Sargent, 2017), defined as the upper bound on the fraction of a worker's output that is allocated to vacancy creation. It is well understood that a small fundamental surplus fraction driven by a large value of b is crucial to deliver realistic volatilities of unemployment and vacancies (Hagedorn and Manovskii, 2008; Ljungqvist and Sargent, 2017). While b affects overall labor market volatility, the matching elasticity, ϕ, affects the relative volatilities of vacancies and unemployment. To see this, we differentiate the steady-state conditions $\bar{u} = \bar{s}(1 - \chi\bar{f})/(\bar{s}(1 - \chi\bar{f}) + \bar{f})$ and $\bar{v} = \bar{\theta}\bar{u}^s$ to

---

[7]Ruge-Murcia (2012) applies SMM to several nonlinear business cycle models and finds that asymptotic standard errors tend to overstate the variability of the estimates. This underscores the importance of using Monte Carlo methods.

[8]We regress each series on its most recent 4 lags following an 8 quarter window. Hodrick (2020) shows this method is more accurate than using a Hodrick and Prescott (1997) filter when series, such as ours, are first-difference stationary.

determine the elasticities of unemployment and vacancies with respect to labor market tightness, θ:

$$\bar{\epsilon}_{u,\theta} = -(1-\bar{u})(1-\phi)/(1-\chi\bar{f}),$$
$$\bar{\epsilon}_{v,\theta} = 1 - (1-\chi\bar{s}/\bar{u}^s)(1-\bar{u})(1-\phi)/(1-\chi\bar{f}).$$

As ϕ increases, the responsiveness of unemployment to changes in labor market tightness shrinks relative to the responsiveness of vacancies. Intuitively, when ϕ is higher, an increase in matches requires a smaller increase in unemployed searching and hence unemployment. Therefore, when matches fluctuate, unemployment fluctuates less relative to vacancies. Thus, we estimate b and ϕ by targeting the standard deviations of detrended unemployment and detrended vacancies in the data.

The Nash bargaining parameter, η, governs the responsiveness of wages to changes in the marginal product of labor, which is driven by labor productivity, $\ell \equiv y/n$. Hence, we follow Hagedorn and Manovskii (2008) and estimate η by targeting the empirical elasticity of detrended wages with respect to detrended labor productivity. The last two labor market parameters, κ and χ, are estimated by targeting the average unemployment and job finding rates.[9] Specifically, we first set $\bar{u}$ and $\bar{s}$ to target the average unemployment and job separation rates in the data and then solve for the vacancy posting cost, κ, and intra-period search duration, χ, using the steady-state conditions:

$$\kappa = \bar{q}(1-\eta)(\bar{a}-b)/(1-\beta(1-\bar{s})),$$
$$\chi = ((1-\bar{u})\bar{s} - \bar{f}\bar{u})/((1-\bar{u})\bar{s}\bar{f}).$$

We set the parameters of the TFP process, ρ_a and $\bar{\sigma}_a$, by targeting the standard deviation and autocorrelation of detrended output. The investment adjustment cost parameter, ν, is identified by targeting the standard deviations and autocorrelations of detrended consumption and investment. The parameters of the TFP volatility process, σ_{sv} and ρ_{sv}, are pinned down by targeting the standard deviation, autocorrelation, and cyclicality of the real uncertainty series in Ludvigson et al. (2021).

5.4 VARIANCE DECOMPOSITIONS METHODS To decompose the variance of a model outcome into its structural components, we use a Total Variance Decomposition (TVD) that builds on the method in Isakin and Ngo (2020). This approach generalizes standard methods such as linear forecast error variance decompositions. Based on the law of total variance, the TVD accounts for model nonlinearities and multiplicative interaction effects that occur between level and volatility shocks.

To demonstrate, let $\varepsilon_t = [\varepsilon_{1,t}, \ldots, \varepsilon_{n,t}]'$ denote a vector of shocks and $y_t = f(y_{t-1}, \varepsilon_t)$ denote the state space representation of an outcome y determined by a possibly nonlinear function f. Our goal is to decompose the variance of the h-step ahead forecast error in period t, $V_t[y_{t+h} - E_t y_{t+h}] = V_t[y_{t+h}]$, into components attributable to each shock and their nonlinear interactions. To achieve

---

[9]Blanchard and Galí (2010) and Leduc and Liu (2016) use a quarterly calibration and set $\chi = 1$, whereas Hagedorn and Manovskii (2008) use a weekly frequency and set $\chi = 0$. Each period in our model is 1 month, so we estimate χ.

this, we consider two TVDs. First, let $\{\varepsilon_{-j}\}_{t+1}^{t+h}$ denote a realization of all shocks except j in periods $t+1$ to $t+h$. Conditioning on this set of shocks and applying the law of total variance yields

$$V_t[y_{t+h}] = E_t[V_t[y_{t+h}|\{\varepsilon_{-j}\}_{t+1}^{t+h}]] + V_t[E_t[y_{t+h}|\{\varepsilon_{-j}\}_{t+1}^{t+h}]]. \tag{18}$$

The first term computes the variance of y_{t+h} driven by the jth shock $\{\varepsilon_j\}_{t+1}^{t+h}$, and then averages over all possible paths of the other shocks $\{\varepsilon_{-j}\}_{t+1}^{t+h}$. Therefore, this term captures the total contribution of shock j to the variance. As emphasized by Isakin and Ngo (2020), this contribution contains both its direct and interaction effects. The second term captures the residual variance due to the other shocks, which includes their direct effects and interactions excluding those with shock j.

To decompose the total effect of shock j into its direct and interaction effects, we extend Isakin and Ngo (2020) and consider a second TVD that conditions on the jth shock, $\{\varepsilon_j\}_{t+1}^{t+h}$. This implies

$$V_t[y_{t+h}] = E_t[V_t[y_{t+h}|\{\varepsilon_j\}_{t+1}^{t+h}]] + V_t[E_t[y_{t+h}|\{\varepsilon_j\}_{t+1}^{t+h}]]. \tag{19}$$

In this case, the first term captures the variance contribution of all shocks except j, including both their direct and interaction effects. More importantly, the second term captures the residual variance driven by only the direct effect of the jth shock. Computing the decompositions in (18) and (19) for each shock $j = 1, \ldots, n$ allows us to parse out the direct and interaction effects of shock j.

Examples To highlight the importance of interaction effects, consider outcome $y_t = f(\varepsilon_{1,t}, \varepsilon_{2,t})$ driven by two independent standard normal shocks $\varepsilon_{1,t}, \varepsilon_{2,t} \sim N(0,1)$. First suppose f is linear so

$$y_t = \sigma_1 \varepsilon_{1,t} + \sigma_2 \varepsilon_{2,t}, \quad \sigma_1, \sigma_2 > 0.$$

Conditioning on each shock and applying the TVD shows that the total contribution of shock $j \in \{1, 2\}$ is σ_j^2 and direct effects account for 100% of the total contributions. In a linear setting, there are never any interaction effects and the sum of the total contributions is equal to the total variance. Therefore, our approach nests the standard linear forecast error variance decomposition.

Second, consider a simple model of stochastic volatility, where

$$y_t = \sigma_t \varepsilon_{1,t}, \quad \sigma_t = \bar{\sigma} + \sigma_{sv} \varepsilon_{2,t}.$$

In this setting, shock 1 directly impacts the level of y_t, while shock 2 only affects y_t through its impact on the volatility of the level shock. Conditioning on shock 1 and applying the TVD yields

$$V_t[y_{t+h}] = E_t[V_t[(\bar{\sigma} + \sigma_{sv}\varepsilon_{2,t+h})\varepsilon_{1,t+h}|\{\varepsilon_1\}_{t+1}^{t+h}]] + V_t[E_t[(\bar{\sigma} + \sigma_{sv}\varepsilon_{2,t+h})\varepsilon_{1,t+h}|\{\varepsilon_1\}_{t+1}^{t+h}]],$$

which simplifies to $V_t[y_{t+h}] = \sigma_{sv}^2 + \bar{\sigma}^2$. Hence, the total contribution of shock 2 is σ_{sv}^2, while the direct effect of shock 1 is $\bar{\sigma}^2$. Conditioning on shock 2 yields $V_t[y_{t+h}] = (\bar{\sigma}^2 + \sigma_{sv}^2) + 0$, so the total

contribution of shock 1 is $\bar{\sigma}^2 + \sigma_{sv}^2$, while the direct effect of shock 2 is zero. The share of shock 1's total variance contribution due to direct effects is $\bar{\sigma}^2/(\bar{\sigma}^2 + \sigma_{sv}^2)$, while shock 2's contribution is entirely driven by interaction effects with shock 1. Note that in this nonlinear setting, the total contributions no longer sum to the total variance due to double counting of the interaction effects.

6 QUANTITATIVE RESULTS

This section shows the parameter estimates and empirical fit of our model. It then quantifies the importance of the endogenous uncertainty mechanism and decomposes its sources and consequences.

Parameter	Mean	SE	Parameter	Mean	SE
Search Duration (χ)	0.5463	0.0011	Investment Adjustment Cost (ν)	5.4153	0.0215
Vacancy Posting Cost (κ)	1.1919	0.0090	TFP Level Shock AC (ρ_a)	0.9239	0.0006
Outside Option (b)	0.9380	0.0003	TFP Level Shock SD ($\bar{\sigma}_a$)	0.0105	0.0000
Matching Elasticity (ϕ)	0.4940	0.0004	TFP Volatility Shock AC (ρ_{sv})	0.9438	0.0008
Bargaining Weight (η)	0.1465	0.0007	TFP Volatility Shock SD (σ_{sv})	0.0149	0.0001

(a) Parameter estimates and standard errors.

Target	Data	SE	Model	Target	Data	SE	Model
$E(u)$	5.97	0.25	5.93	$SD(\mathcal{U})$	5.93	0.62	6.06
$E(f)$	41.88	1.26	41.92	$AC(\mathcal{U})$	0.89	0.04	0.89
$SD(\tilde{y})$	3.15	0.31	3.65	$Corr(\mathcal{U}, \tilde{y})$	-0.60	0.08	-0.62
$SD(\tilde{c})$	2.06	0.17	2.01	$AC(\tilde{y})$	0.90	0.03	0.88
$SD(\tilde{\imath})$	8.68	0.82	7.30	$AC(\tilde{c})$	0.88	0.03	0.92
$SD(\tilde{u})$	21.36	1.98	21.14	$AC(\tilde{\imath})$	0.89	0.04	0.86
$SD(\tilde{v})$	21.64	2.08	21.65	$Slope(\tilde{w}, \tilde{\ell}_p)$	0.63	0.09	0.63

(b) Data and simulated moments. The overall fit is $J = 8.76$ with p-value 0.067.

Table 2: Estimation results.

6.1 EMPIRICAL FIT   Table 2a shows the parameters, which are precisely estimated and within conventional ranges. The matching elasticity, ϕ, is in the range of elasticities estimated in the data (Mortensen and Nagypal, 2007; Petrongolo and Pissarides, 2001). The outside option, b, is close to the value in Hagedorn and Manovskii (2008), while the vacancy posting cost κ implies that vacancy creation costs about 1% of output in steady state. The estimate for χ implies that newly separated workers have on average about half a month to find a new job before being recorded as unemployed (Shimer, 2005). The estimate for ν implies that capital adjustment costs are small ($< 0.1\%$ of output in the ergodic distribution), although they are important for matching investment dynamics.

Overall, the small standard errors indicate the strength of our identification scheme. In particular, the data pins down the TFP volatility process, which is crucial for decomposing uncertainty.

The success of our estimation is also clear from the simulated moments. Table 2b reports the mean and standard errors of the target moments as well as the simulated moments based on the mean parameter estimates. Importantly, the model matches the standard deviation and autocorrelation of uncertainty as well as its correlation with output. In addition, the model closely matches all of the real activity and labor moments. The fit is sufficiently strong that the model passes an over-identifying restrictions test at the 5% confidence level. These results provide confidence that the DMP model provides a credible description of real activity and uncertainty over the business cycle.

Our model's ability to generate realistic uncertainty dynamics does not require a specific theory of labor market volatility. Given realistic labor market volatility, the nonlinearity in the law of motion for employment generates realistic uncertainty dynamics. While we follow Hagedorn and Manovskii (2008) by setting the outside option b to match labor market volatility, Ljungqvist and Sargent (2017) show that alternative protocols such as sticky wages or alternating offer bargaining also deliver realistic labor market volatility. Furthermore, Appendix F shows that extending our model to include home production (Benhabib et al., 1991; Petrosky-Nadeau et al., 2018) also allows it to generate realistic labor market volatility and hence countercyclical uncertainty dynamics.

	Output	Uncertainty
Level Total	100.00	43.50
Volatility Total	0.20	57.01
Level Direct	99.80	42.99
Volatility Direct	0.00	56.50

Table 3: Variance decompositions

	Mode	Recession	% Change
Match Value ($\lambda_n^{(1-\phi)/\phi}$)	9.52	8.94	-6.15
Finding Rate (f)	9.52	8.94	-6.09
Employment ($\ln n$)	0.46	0.91	95.16
Output ($\ln y$)	1.98	2.23	12.45

Table 4: Conditional standard deviations

6.2 QUANTIFYING THE MECHANISM   The endogenous uncertainty mechanism is responsible for the negative correlation between output and uncertainty in our model. To see this, Table 3 reports variance decompositions of output and uncertainty. Exogenous volatility shocks explain 57% of the variance in uncertainty but none of the variance in output. Level shocks explain almost 100% of the variance in output and 43% of the variance in uncertainty. Thus, the negative correlation between uncertainty and output must be driven by an response of uncertainty to first moment shocks.

To visualize the model's dynamics, Figure 2 plots generalized impulse responses of unemployment and uncertainty to 2 standard deviation positive level and volatility shocks.[10] The economy is initialized at the ergodic mean, but the responses are qualitatively the same when it begins in other states. In line with the variance decompositions in Table 3, both variables strongly respond to the level shock, but only uncertainty significantly responds to the volatility shock. These results provide another way to see that most of the countercyclical fluctuations in uncertainty are endogenous.

---

[10]Following Koop et al. (1996), the response of x_{t+h} over horizon h is given by $\mathcal{G}_t(x_{t+h}|\varepsilon_{sv,t+1} = 2, \mathbf{z}_t) = 100 \times (E_t[x_{t+h}|\varepsilon_{sv,t+1} = 2, \mathbf{z}_t] - E_t[x_{t+h}|\mathbf{z}_t])$, where $\mathbf{z}_t$ is the state vector and 2 is the shock size in period $t + 1$.
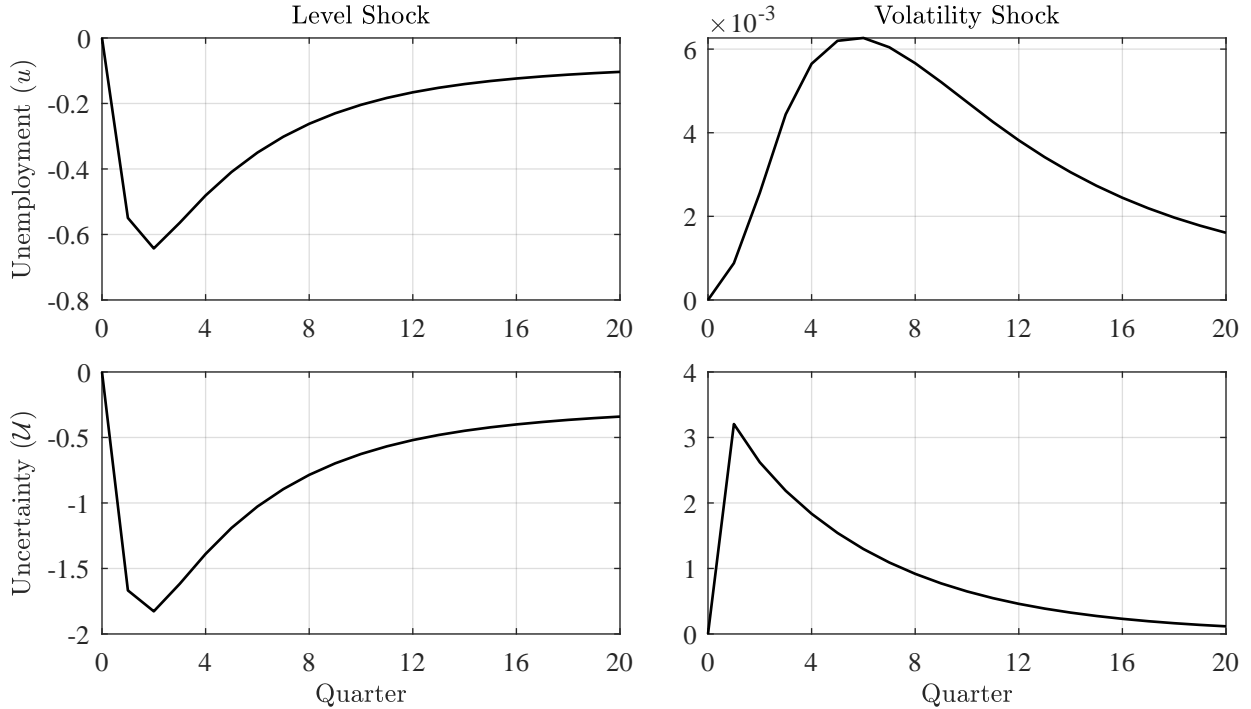
Figure 2: Generalized impulse responses to 2 standard deviation positive level and volatility shocks. The unemployment rate is a percentage point deviation from the baseline, while uncertainty is the change in levels.

Sources of Uncertainty We use the insights in Section 4 to quantify the drivers of the countercyclicality. Table 4 reports the conditional standard deviations of key variables—the match value, the job finding rate, employment, and output—when the economy begins at the ergodic mode ($u_0 = 5\%$) and a recession ($u_0 = 10\%$).[11] The last column shows the percent change across the two states.

Our quantitative model relaxes the assumptions used in Section 4 to derive $\lambda_{n,t+1}$ in closed form. In particular, the dynamics of $\lambda_{n,t+1}$ are mainly driven by the marginal product of labor, $(1-\alpha)a_{t+1}(k_t/n_{t+1})^\alpha$, which is increasing in TFP but decreasing in employment. This means the responsiveness of $\lambda_{n,t+1}$ to shocks is larger when the response of employment is smaller, which occurs when unemployment is lower. Therefore, uncertainty about $\lambda_{n,t+1}$ falls by 6% in the recession state and is not the source of the countercyclicality. Uncertainty about the job finding rate decreases by about the same amount as match value uncertainty because the two quantities are proportional.

Consistent with our analytical results, employment uncertainty significantly increases in recessions and is the primary driver of the countercyclicality of uncertainty. This feeds into output uncertainty through the production function. The level change in output uncertainty across the two states is roughly equal to the change in employment uncertainty scaled by the cost share of labor.

---

[11]We simulate the model for a large number of periods, burning off the first 1,000 periods. The initial state is equal to the average across periods where the unemployment rate is within 25 basis points of u_0. To compute the conditional standard deviations in Table 4, we conduct $10,000$ $h = 3$ period ahead Monte Carlo simulations from each initial state.

Mechanism Evidence   Our model endogenously generates countercyclical uncertainty because search and matching frictions make uncertainty about future matches increasing in unemployment. As shown in Section 4, this mechanism is immediate when inflows to employment are written in terms of the job finding rate, $m_{t+1} = f_{t+1} u^s_{t+1}$, which is a standard accounting identity commonly used in the literature. Nonetheless, to provide direct evidence for the mechanism, we follow the estimation approach in Jurado et al. (2015) and compute empirical uncertainty series for the inflows to employment, m_t, and the job finding rate, f_t.[12] We then compute the correlation of each uncertainty series with the level of unemployment and compare them to their model-based counterparts.

In the data, the correlation between match (i.e., employment inflow) uncertainty and unemployment is 0.83, while the correlation between finding rate uncertainty and unemployment is -0.34. These moments are consistent with their model-implied counterparts: the correlations of match uncertainty and finding rate uncertainty with unemployment in the model are 0.96 and -0.14, respectively. This suggests that the uncertainty dynamics implied by the model are borne out empirically.

What about Capital Adjustment Costs?   The countercyclical uncertainty mechanism operates in a similar manner to a countercyclical adjustment cost in the law of motion for employment. When unemployment is higher, new matches respond more to the job finding rate, which is indicative of lower employment adjustment costs. Given this connection, it is useful to check whether adjustment costs in the law of motion for capital also generate countercyclical uncertainty fluctuations.[13]

To investigate whether capital adjustment costs generate time-varying endogenous uncertainty, Appendix G studies calibrated Real Business Cycle and New Keynesian models. In both models, uncertainty is almost entirely driven by exogenous volatility shocks, so the correlation between output and uncertainty is near zero. Therefore, standard capital adjustment costs are insufficient to generate countercyclical uncertainty, confirming the importance of search and matching frictions.

6.3   VOLATILITY SHOCK SIZE   Our identification strategy produced a small standard deviation for the uncertainty shock. Others have worked with models where this standard deviation is much larger. We investigate how this affects our conclusions about the strength of the endogenous uncertainty mechanism. Formally, we set $\sigma_{sv} = 0.3543$, so a one standard deviation increase in $\sigma_{a,t}$ doubles its mean value. This value is similar to the values in Leduc and Liu (2016) and Fernández-Villaverde and Guerrón-Quintana (2020). Given σ_{sv}, we recalibrate $\bar{\sigma}_a = 0.0032$ to target the standard deviation of detrended output. As a result, the fluctuations in TFP volatility increase, but average TFP volatility decreases by about 70%. Other parameters are held at their estimated values.

Table 5 shows key data and model-implied moments. While the standard deviations of output

---

[12]We take level differences of both series to render them stationary and add them to the FAVAR used to compute the real uncertainty series. We then extract the individual uncertainty series for the inflows to employment and vacancies.

[13]We focus on capital adjustment costs within the representative firm paradigm. A recent literature shows that adjustment costs create a role for uncertainty shocks when firms are heterogeneous (Bloom, 2009; Bloom et al., 2018).

Moment	Data	Large σ_{sv}	No Vol. Shocks
$SD(\mathcal{U})$	5.93	90.15	1.21
$SD(\tilde{y})$	3.15	3.15	1.11
$SD(\tilde{u})$	21.36	17.43	6.46
$Corr(\mathcal{U}, \tilde{y})$	−0.60	−0.04	−0.95

Table 5: Key Moments

Contribution	Output	Uncertainty
Level Total	99.57	2.30
Volatility Total	65.55	99.95
Level Direct	34.45	0.05
Volatility Direct	0.43	97.70

Table 6: Large σ_{sv} variance decomposition

and unemployment remain close to the data, the standard deviation of uncertainty is much larger than our preferred empirical measure, reflecting the larger value of σ_{sv}. Furthermore, its correlation with output almost completely disappears. The smaller correlation is due to the different transmission of volatility shocks to output and uncertainty. When we compute the model-implied moments with the exogenous uncertainty shocks turned off, uncertainty volatility sharply declines and there is a strong negative correlation between uncertainty and output. This shows that search and matching frictions are the source of the countercyclicality, even with a much larger shock size.

Table 6 shows the variance decompositions of output and uncertainty. Starting with output, level shocks account for almost 100% of the variance and volatility shocks account for around 66%, suggesting that volatility shocks are a key contributor to business cycle fluctuations. However, the decomposition reveals that direct level effects account for about 34% of the total variance, while direct volatility effects account for less than 1%. Hence, the transmission of volatility shocks to output is almost entirely due to their interaction with level shocks. Direct effects of volatility shocks that operate through channels such as precautionary savings have relatively small effects on output, even though they generate impulse responses of unemployment that are 10 times larger than in Figure 2 and are similar to the responses in Leduc and Liu (2016) and Freund and Rendahl (2020).

The exogenous volatility shocks transmit to uncertainty almost entirely through direct effects, which account for nearly 100% of the uncertainty variance. This shows the fluctuations in uncertainty are mostly exogenous in this case, unrelated to level shocks or output fluctuations. The larger volatility shocks dilute the endogenous mechanism and lower the countercyclicality of uncertainty.

6.4 CONSEQUENCES OF ENDOGENOUS UNCERTAINTY   In our model, there is little feedback from the endogenous fluctuations in uncertainty to real activity. To see this, Table 7 shows the results of two comparisons. First, column 3 reports moments from a log-linear version of our model in which there are no fluctuations in endogenous uncertainty. The volatilities of output and unemployment are essentially unchanged, indicating that they are unaffected by the presence of endogenous uncertainty. Second, column 4 shows the moments after shutting off exogenous volatility shocks like we did for the alternative calibration in Table 5.[14] Removing these shocks lowers the

---

[14]We also estimated the model without volatility shocks or targeting uncertainty dynamics. The model closely matches the data. The implied values of $SD(\mathcal{U})$ and $Corr(\mathcal{U}, \tilde{y})$ were 3.99 and −0.98, similar to column 4 of Table 7.

Moment	Data	Baseline	Log-Linear	No Vol. Shocks	Hosios
$SD(\mathcal{U})$	5.93	6.06	0.00	3.86	7.38
$SD(\tilde{y})$	3.15	3.65	3.57	3.66	3.79
$SD(\tilde{u})$	21.36	21.14	22.79	21.16	22.95
$Corr(\mathcal{U}, \tilde{y})$	-0.60	-0.62	0.00	-0.98	-0.72

Table 7: Key moments in the data and DMP model. "Baseline" is the estimated model; "Log-linear" linearizes the entire model; "No Vol. Shocks" turns off the volatility shocks. "Hosios" is the efficient solution.

standard deviation of uncertainty and pushes its correlation with output towards -1. These results emphasize the strength of the search and matching mechanism and show that exogenous volatility shocks are essential for matching the data because they increase $SD(\mathcal{U})$ and weaken $Corr(\mathcal{U}, \tilde{y})$.

Finally, we note that the endogenous fluctuations in uncertainty are an artifact of search and matching frictions that survives even when the economy is constrained efficient. We see this by comparing column two to the final column where we solve the model under the Hosios (1990) condition ($\eta = \phi$), which ensures constrained efficiency of the equilibrium allocation.[15] There are only minor changes in the volatilities of uncertainty and output, suggesting that any efficient policy intervention in the estimated model would have only a minor impact on the dynamics of uncertainty. In fact, efficient policy design would not even focus on stabilizing the endogenous fluctuations in uncertainty. It would simply aim to make firms' vacancy posting decisions efficient.

These properties contrast with the literature on the real effects of uncertainty shocks and leading explanations of countercyclical uncertainty. For example, Fajgelbaum et al. (2017) propose an information-based mechanism in which endogenous fluctuations in uncertainty cause recessions. In our model, endogenous uncertainty has little effect on real activity and policy has a minor role.

6.5 VAR IMPLICATIONS   The literature often uses recursive identification schemes in structural VARs to identify the effect of aggregate uncertainty shocks on real activity.[16] Through the lens of our estimated DMP model, countercyclical fluctuations in uncertainty are endogenous responses to changes in real activity. Therefore, a recursive identification scheme that places uncertainty before a measure of real activity will not be able to properly identify the structural shocks in our model.

To illustrate this, Appendix I shows the results from estimating a bivariate VAR with actual and simulated data from the model. When uncertainty is ordered first, the actual and simulated VAR responses to an uncertainty shock are similar, even though we know the true structural uncertainty shocks have almost no impact on output in our model. This occurs because the uncertainty shock in the VAR is correlated with both the level and uncertainty shock from the estimated DMP model.

---

[15]Appendix H proves that the original Hosios (1990) condition is unchanged in our search and matching model.

[16]See, for example, Bachmann et al. (2013), Basu and Bundick (2017), Bekaert et al. (2013), Bloom (2009), Fernández-Villaverde et al. (2015), Gilchrist et al. (2014), Jurado et al. (2015), Leduc and Liu (2016), and Oh (2020).

7 EXTENSIONS

This section enriches our baseline model with features that could alter the strength of the endogenous uncertainty mechanism. For clarity, each extension is considered separately. In each case, we find that search and matching frictions remain the dominant source of countercyclical uncertainty.

7.1 MODEL EXTENSIONS

We consider five extensions to our estimated model. First, we separate risk aversion, γ, from the elasticity of intertemporal substitution, ψ, by endowing the household with Epstein and Zin (1989, 1991) preferences. The utility function and pricing kernel become

$$J_t^H = ((1-\beta)c^{1-1/\psi} + \beta E_t[(J_{t+1}^H)^{1-\gamma}]^{(1-1/\psi)/(1-\gamma)})^{1/(1-1/\psi)},$$
$$x_{t+1} = \beta(c_t/c_{t+1})^{1/\psi}(J_{t+1}^{1-\gamma}/E_t[(J_{t+1}^H)^{1-\gamma}])^{(1/\psi-\gamma)/(1-\gamma)}.$$

This extension helps us evaluate the effects of having a stronger motive for precautionary savings.

Second, we incorporate a New Keynesian block due to the prominence of nominal rigidities in the literature (e.g. Born and Pfeifer, 2014; Fernández-Villaverde et al., 2015; Freund and Rendahl, 2020; Leduc and Liu, 2016; Mumtaz and Zanetti, 2013). This extension replaces (11) and (12) with

$$r_t^k = \alpha mc_t y_t/k_{t-1},$$
$$\lambda_{n,t} = (1-\alpha)mc_t y_t/n_t - w_t + (1-\bar{s})E_t[x_{t+1}\lambda_{n,t+1}],$$

where mc_t denotes marginal cost. It also adds a Phillips curve, bond Euler equation, and Taylor rule

$$\varphi(\pi_t/\bar{\pi} - 1)(\pi_t/\bar{\pi}) = 1 - \theta + \theta mc_t + \varphi E_t[x_{t+1}(\pi_{t+1}/\bar{\pi} - 1)(\pi_{t+1}/\bar{\pi})y_{t+1}/y_t,$$
$$1 = E_t[x_{t+1}(r_t/\pi_{t+1})],$$
$$r_t = \bar{r}(\pi_t/\bar{\pi})^{\phi_\pi},$$

where r_t is the gross nominal interest rate, $\pi_t = p_t/p_{t-1}$ is the gross inflation rate, $\theta > 1$ is the elasticity of substitution between intermediate goods, and $\varphi > 0$ scales the price adjustment cost.

Third, we add downward wage rigidity (DWR) as an extra source of nonlinearity (Abbritti and Fahr, 2013; Cacciatore and Ravenna, 2021; Dupraz et al., 2019). The wage protocol, (15), becomes

$$w_t = \max\{\eta((1-\alpha)y_t/n_t + \kappa(1-\chi\bar{s})E_t[x_{t+1}\theta_{t+1}]) + (1-\eta)b, w_m\},$$

where w_m is the minimum real wage rate. When $w_t = w_m$, firms face lower profits, so the job finding rate becomes concave in TFP and exhibits larger declines in response to negative TFP shocks.

Fourth, we introduce inelastic vacancy creation. Vacancies are important since they influence employment dynamics through unemployment. In our baseline model, vacancy creation is infinitely elastic. To relax this, we follow Coles and Kelishomi (2018) and add convex vacancy costs,

$\kappa_i v_t^{1+1/\nu_v}/(1+1/\nu_v)$, where ν_v is the elasticity of vacancy creation. With $\kappa = 0$, (12)-(16) become

$$w_t = \eta(w_{f,t} + (1 - \chi\bar{s})E_t[x_{t+1}\theta_{t+1}\kappa_i v_{t+1}^{1/\nu_v}]) + (1 - \eta)b,$$

$$\frac{\kappa_i v_t^{1/\nu_v}}{q_t} = w_{f,t} - w_t + (1 - \bar{s})E_t[x_{t+1}\frac{\kappa_i v_{t+1}^{1/\nu_v}}{q_{t+1}}],$$

$$c_t + i_t + \frac{\kappa_i}{1+1/\nu_v}v_t^{1+1/\nu_v} = y_t.$$

Fifth, we introduce endogenous job separations (EJS) following Den Haan et al. (2000). This extension allows us to match the mean and standard deviation of the job separation rate in the data.

Final good firms choose capital k_{t-1} and effective labor ℓ_t to maximize $y_t - r_t^k k_{t-1} - w_{f,t}\ell_t$ with $y_t = a_t k_{t-1}^\alpha \ell_t^{1-\alpha}$. Effective labor is $\ell_t = ((1-\bar{s})n_{t-1} + q_t v_t)\int_{\underline{z}_t}^\infty z_t dF(z_t)$, where $(1-\bar{s})n_{t-1} + q_t v_t$ is the mass of matched workers in period t and z_t is an idiosyncratic level of worker efficiency with cumulative distribution function (CDF), $F(z_t)$. Only workers with $z_t \geq \underline{z}_t$ actually produce. The mass $F(\underline{z}_t)((1-\bar{s})n_{t-1} + q_t v_t)$ are endogenously separated before production occurs in period t.

Workers are hired by employment agencies who solve

$$J_t^E = \max_{n_t, v_t, \underline{z}_t} ((1 - \bar{s})n_{t-1} + q_t v_t)\int_{\underline{z}_t}^\infty (w_{f,t}z_t - w_t(z_t))dF(z_t) - \kappa v_t + E_t x_{t+1}J_{t+1}^E$$

subject to

$$n_t = (1 - F(\underline{z}_t))((1 - \bar{s})n_{t-1} + q_t v_t),$$

$$v_t \geq 0.$$

Appendix L shows the entire equilibrium system. To compute $F(\underline{z}_t)$ and $\int_{\underline{z}_t}^\infty z_t dF(z_t)$, we assume that $\ln z_t \sim \mathbb{N}(-\sigma_z^2/2, \sigma_z^2)$. Letting Φ denote the CDF of a standard normal distribution, we obtain

$$F(\underline{z}_t) = \Phi\left(\frac{\ln \underline{z}_t + \sigma_z^2/2}{\sigma_z}\right), \quad G(\underline{z}_t) \equiv \int_{\underline{z}_t}^\infty z_t dF(z_t) = 1 - \Phi\left(\frac{\ln \underline{z}_t - \sigma_z^2/2}{\sigma_z}\right).$$

Finally, as an additional robustness check, we introduce endogenous search intensity to the baseline DMP model following Leduc and Liu (2020). Appendix J describes the model and results.

7.2 QUANTITATIVE RESULTS   We set the new parameters in line with the literature, though our results do not depend on these values. When we allow for Epstein-Zin preferences, we set the coefficient of relative risk aversion, γ, to 80 and the elasticity of intertemporal substitution, ψ, to 2.

In the NK extension, we set the elasticity of substitution between intermediate goods, θ, to 11, so there is a 10% steady-state markup. The Rotemberg price adjustment cost parameter, φ, is set to 400 to produce a Phillips curve with slope 0.025. The monetary response to inflation, ϕ_π, is set to 2.

In the model with downward wage rigidity, we follow Cacciatore and Ravenna (2021) and calibrate w_m to truncate the bottom 5% of the wage distribution in the economy without the constraint.

The model with vacancy adjustment costs lowers the volatility of unemployment, which makes

it difficult to compare to the other model extensions. Therefore, we assume quadratic costs ($\nu_v = 1$) and restore labor market volatility by raising b to 0.96 following Hagedorn and Manovskii (2008).

In the model with endogenous job separations, there is an additional source of endogenous volatility driven by the effective job separation rate $s_t = \bar{s} + (1 - \bar{s})F(\underline{z}_t)$. We set $\bar{s}$ and σ_z to target the mean and standard deviation of the job separation rate, which is constructed by following Shimer (2012). Conditional on those values, we set $\bar{\sigma}_a$ to target the standard deviation of detrended output in the data. All other parameters in each model are fixed at the estimated values in Table 2.

	DMP	+EZ	+NK	+DWR	+IVC	+EJS
Key Moments						
$SD(\mathcal{U})$	6.06	6.12	7.26	7.38	7.20	9.76
$SD(\tilde{y})$	3.65	3.61	3.67	3.76	3.63	3.18
$SD(\tilde{u})$	21.21	20.80	20.89	22.58	19.54	22.21
$Corr(\mathcal{U}, \tilde{y})$	-0.62	-0.62	-0.71	-0.71	-0.68	-0.81
$SD(\tilde{s})$	0.00	0.00	0.00	0.00	0.00	8.48
Output Decomposition						
TFP Level Total	100.00	100.00	100.00	100.00	100.00	100.00
TFP Volatility Total	0.20	0.20	0.23	0.21	0.21	0.24
TFP Level Direct	99.80	99.80	99.77	99.79	99.79	99.76
TFP Volatility Direct	0.00	0.00	0.00	0.00	0.00	0.00
Uncertainty Decomposition						
TFP Level Total	43.50	41.84	57.86	60.89	58.06	75.59
TFP Volatility Total	57.01	58.43	42.63	39.53	42.70	25.01
TFP Level Direct	42.99	41.57	57.37	60.47	57.30	74.99
TFP Volatility Direct	56.50	58.16	42.14	39.11	41.94	24.41

Table 8: Key moments and variance decompositions. +EZ introduces Epstein-Zin preferences, +NK adds New Keynesian nominal rigidities, +DWR adds downward nominal wage rigidity, +IVC introduces inelastic vacancy creation, and +EJS adds endogenous job separations to the estimated DMP model. In the data, $SD(\mathcal{U}) = 5.93$, $SD(\tilde{y}) = 3.15$, $SD(\tilde{u}) = 21.36$, $Corr(\mathcal{U}, \tilde{y}) = -0.60$, $E(s) = 3.28$, and $SD(s) = 8.61$.

Variance Decomposition Table 8 shows the key moments as well as our variance decomposition. The standard deviations of output and variance decompositions are similar to the baseline model. However, each extension generates a higher standard deviation of uncertainty than the baseline model. They also typically attribute a larger variance share to level shocks, which is indicative of more endogenous uncertainty. The greater the increase in time-varying uncertainty, the stronger the negative correlation between uncertainty and output, so the additional uncertainty is also countercyclical. These results suggest that richer DMP models will either have little effect or amplify the search and matching mechanism that drives countercyclical uncertainty in the baseline model.[17]

---

[17]Appendix K shows impulse responses of output and uncertainty to level and volatility shocks in each extension.

8 CONCLUSION

This paper shows that search and matching frictions can endogenously explain the negative correlation between output and real uncertainty because the inherent nonlinearity in the flow of new matches makes employment uncertainty increasing in the number of people searching for work. Quantitatively, this mechanism is strong enough to explain uncertainty and real activity dynamics, including their correlation. Through this lens, uncertainty fluctuations are endogenous responses to changes in real activity, and the results are robust to several popular extensions to the DMP model.

In contrast with other mechanisms in the literature, the endogenous uncertainty fluctuations from the search and matching mechanism do not feed back into real activity dynamics. They also remain when the economy is constrained efficient, suggesting that there is little role for policy. Given the novelty of our results, we chose to focus on real uncertainty. Extending our analysis to financial uncertainty and its relationship with real activity is an important area for future research.

REFERENCES

ABBRITTI, M. AND S. FAHR (2013): "Downward Wage Rigidity and Business Cycle Asymmetries," *Journal of Monetary Economics*, 60, 871–886, https://doi.org/10.1016/j.jmoneco.2013.08.001.

ANDOLFATTO, D. (1996): "Business Cycles and Labor-Market Search," *American Economic Review*, 86, 112–132.

ARELLANO, C., Y. BAI, AND P. J. KEHOE (2019): "Financial Frictions and Fluctuations in Volatility," *Journal of Political Economy*, 127, 2049–2103, https://doi.org/10.1086/701792.

ATKINSON, T., M. PLANTE, A. W. RICHTER, AND N. A. THROCKMORTON (2022): "Complementarity and Macroeconomic Uncertainty," *Review of Economic Dynamics*, 44, 225–243, https://doi.org/10.1016/j.red.2021.03.003.

BACHMANN, R. AND C. BAYER (2013): "'Wait-and-See' Business Cycles?" *Journal of Monetary Economics*, 60, 704–719, https://doi.org/10.1016/j.jmoneco.2013.05.005.

BACHMANN, R., S. ELSTNER, AND E. SIMS (2013): "Uncertainty and Economic Activity: Evidence from Business Survey Data," *American Economic Journal: Macroeconomics*, 5, 217–49, https://doi.org/10.1257/mac.5.2.217.

BARNICHON, R. (2010): "Building a Composite Help-Wanted Index," *Economics Letters*, 109, 175–178, https://doi.org/10.1016/j.econlet.2010.08.029.

BASU, S. AND B. BUNDICK (2017): "Uncertainty Shocks in a Model of Effective Demand," *Econometrica*, 85, 937–958, https://doi.org/10.3982/ECTA13960.

BEKAERT, G., M. HOEROVA, AND M. LO DUCA (2013): "Risk, Uncertainty and Monetary Policy," *Journal of Monetary Economics*, 60, 771–788, https://doi.org/10.1016/j.jmoneco.2013.06.003.

BENHABIB, J., X. LIU, AND P. WANG (2016): "Endogenous Information Acquisition and Countercyclical Uncertainty," *Journal of Economic Theory*, 165, 601–642, https://doi.org/10.1016/j.jet.2016.07.007.

BENHABIB, J., R. ROGERSON, AND R. WRIGHT (1991): "Homework in Macroeconomics: Household Production and Aggregate Fluctuations," *Journal of Political Economy*, 99, 1166–1187, https://doi.org/10.1086/261796.

BERGER, D., I. DEW-BECKER, AND S. GIGLIO (2020): "Uncertainty Shocks as Second-Moment News Shocks," *Review of Economic Studies*, 87, 40–76, https://doi.org/10.1093/restud/rdz010.

BERNSTEIN, J., A. W. RICHTER, AND N. A. THROCKMORTON (2022): "The Matching Function and Nonlinear Business Cycles," Federal Reserve Bank of Dallas Working Paper 2201, https://doi.org/10.24149/wp2201.

BIANCHI, F., C. L. ILUT, AND M. SCHNEIDER (2018): "Uncertainty Shocks, Asset Supply and Pricing over the Business Cycle," *Review of Economic Studies*, 85, 810–854, https://doi.org/10.1093/restud/rdx035.

BLANCHARD, O. AND J. GALÍ (2010): "Labor Markets and Monetary Policy: A New Keynesian Model with Unemployment," *American Economic Journal: Macroeconomics*, 2, 1–30, https://doi.org/10.1257/mac.2.2.1.

BLOOM, N. (2007): "Uncertainty and the Dynamics of R&D," *American Economic Review*, 97, 250–255, https://doi.org/10.1257/aer.97.2.250.

——— (2009): "The Impact of Uncertainty Shocks," *Econometrica*, 77, 623–685, https://doi.org/10.3982/ECTA6248.

BLOOM, N., M. FLOETOTTO, N. JAIMOVICH, I. SAPORTA-EKSTEN, AND S. J. TERRY (2018): "Really Uncertain Business Cycles," *Econometrica*, 86, 1031–1065, https://doi.org/10.3982/ECTA10927.

BORN, B. AND J. PFEIFER (2014): "Policy Risk and the Business Cycle," *Journal of Monetary Economics*, 68, 68–85, https://doi.org/10.1016/j.jmoneco.2014.07.012.

CACCIATORE, M. AND F. RAVENNA (2021): "Uncertainty, Wages, and the Business Cycle," *Economic Journal*, 131, 2797–2823, https://doi.org/10.1093/ej/ueab019.

CAGGIANO, G., E. CASTELNUOVO, S. DELRIO, AND R. KIMA (2021): "Financial uncertainty and real activity: The good, the bad, and the ugly," *European Economic Review*, 136, https://doi.org/10.1016/j.euroecorev.2021.

CALDARA, D., C. FUENTES-ALBERO, S. GILCHRIST, AND E. ZAKRAJŠEK (2016): "The Macroeconomic Impact of Financial and Uncertainty Shocks," *European Economic Review*, 88, 185–207, https://doi.org/10.1016/j.euroecorev.2016.02.020.

CESA-BIANCHI, A. AND E. FERNANDEZ-CORUGEDO (2018): "Uncertainty, Financial Frictions, and Nominal Rigidities: A Quantitative Investigation," *Journal of Money, Credit and Banking*, 50, 603–636, https://doi.org/10.1111/jmcb.12505.

CHETTY, R., A. GUREN, D. MANOLI, AND A. WEBER (2012): "Does Indivisible Labor Explain the Difference between Micro and Macro Elasticities? A Meta-Analysis of Extensive Margin Elasticities," in *NBER Macroeconomics Annual 2012, Volume 27*, ed. by D. Acemoglu, J. Parker, and M. Woodford, MIT Press, Cambridge, 1–56.

CHRISTIANO, L. J., R. MOTTO, AND M. ROSTAGNO (2014): "Risk Shocks," *American Economic Review*, 104, 27–65, https://doi.org/10.1257/aer.104.1.27.

CHUGH, S. K. (2016): "Firm Risk and Leverage Based Business Cycles," *Review of Economic Dynamics*, 20, 111–131, https://doi.org/10.1016/j.red.2016.02.001.

COLEMAN, II, W. J. (1991): "Equilibrium in a Production Economy with an Income Tax," *Econometrica*, 59, 1091–1104, https://doi.org/10.2307/2938175.

COLES, M. G. AND A. M. KELISHOMI (2018): "Do Job Destruction Shocks Matter in the Theory of Unemployment?" *American Economic Journal: Macroeconomics*, 10, 118–136, https://doi.org/10.1257/mac.20150040.

DEN HAAN, W. J., G. RAMEY, AND J. WATSON (2000): "Job Destruction and Propagation of Shocks," *American Economic Review*, 90, 482–498, https://doi.org/10.1257/aer.90.3.482.

DUPRAZ, S., E. NAKAMURA, AND J. STEINSSON (2019): "A Plucking Model of Business Cycles," NBER Working Paper 26351, https://doi.org/10.3386/w26351.

ELSBY, M. W. L., G. SOLON, AND R. MICHAELS (2009): "The Ins and Outs of Cyclical Unemployment," *American Economic Journal: Macroeconomics*, 1, 84–110, https://doi.org/10.1257/mac.1.1.84.

EPSTEIN, L. G. AND S. E. ZIN (1989): "Substitution, risk aversion, and the temporal behavior of consumption and asset returns: A theoretical framework," *Econometrica*, 57, 937–69, https://www.doi.org/10.2307/1913778.

——— (1991): "Substitution, risk aversion, and the temporal behavior of consumption and asset returns: An empirical analysis," *Journal of Political Economy*, 99, 263–86, https://doi.org/10.1086/261750.

FAJGELBAUM, P., M. TASCHEREAU-DUMOUCHEL, AND E. SCHAAL (2017): "Uncertainty Traps," *The Quarterly Journal of Economics*, 132, 1641–1692, https://doi.org/10.1093/qje/qjx021.

FERNÁNDEZ-VILLAVERDE, J. AND P. GUERRÓN-QUINTANA (2020): "Uncertainty Shocks and Business Cycle Research," *Review of Economic Dynamics*, 37, S118–S146, https://doi.org/10.1016/j.red.2020.06.005.

FERNÁNDEZ-VILLAVERDE, J., P. GUERRÓN-QUINTANA, K. KUESTER, AND J. F. RUBIO-RAMÍREZ (2015): "Fiscal Volatility Shocks and Economic Activity," *American Economic Review*, 105, 3352–84, https://doi.org/10.1257/aer.20121236.

FERNÁNDEZ-VILLAVERDE, J., P. GUERRÓN-QUINTANA, J. F. RUBIO-RAMÍREZ, AND M. URIBE (2011): "Risk Matters: The Real Effects of Volatility Shocks," *American Economic Review*, 101, 2530–61, https://doi.org/10.1257/aer.101.6.2530.

FREUND, L. AND P. RENDAHL (2020): "Unexpected Effects: Uncertainty, Unemployment, and Inflation," CEPR Discussion Paper 14690.

GARCIA, C. B. AND W. I. ZANGWILL (1981): *Pathways to Solutions, Fixed Points and Equilibria*, Prentice-Hall series in computational mathematics, Prentice-Hall.

GILCHRIST, S., J. W. SIM, AND E. ZAKRAJŠEK (2014): "Uncertainty, Financial Frictions, and Investment Dynamics," NBER Working Paper 20038, https://doi.org/10.3386/w20038.

HAGEDORN, M. AND I. MANOVSKII (2008): "The Cyclical Behavior of Equilibrium Unemployment and Vacancies Revisited," *American Economic Review*, 98, 1692–1706, https://doi.org/10.1257/aer.98.4.1692.

HAMILTON, J. D. (2018): "Why You Should Never Use the Hodrick-Prescott Filter," *Review of Economics and Statistics*, 100, 831–843, https://doi.org/10.1162/rest_a_00706.

HODRICK, R. J. (2020): "An Exploration of Trend-Cycle Decomposition Methodologies in Simulated Data," NBER Working Paper 26750, https://doi.org/10.3386/w26750.

HODRICK, R. J. AND E. C. PRESCOTT (1997): "Postwar U.S. Business Cycles: An Empirical Investigation," *Journal of Money, Credit and Banking*, 29, 1–16, https://doi.org/10.2307/2953682.

HOSIOS, A. J. (1990): "On The Efficiency of Matching and Related Models of Search and Unemployment," *Review of Economic Studies*, 57, 279–298, https://doi.org/10.2307/2297382.

ILUT, C., M. KEHRIG, AND M. SCHNEIDER (2018): "Slow to Hire, Quick to Fire: Employment Dynamics with Asymmetric Responses to News," *Journal of Political Economy*, 126, 2011–2071, https://doi.org/10.1086/699189.

ILUT, C. L. AND M. SCHNEIDER (2014): "Ambiguous Business Cycles," *American Economic Review*, 104, 2368–2399, https://doi.org/10.1257/aer.104.8.2368.

ISAKIN, M. AND P. V. NGO (2020): "Variance Decomposition Analysis for Nonlinear Economic Models," *Oxford Bulletin of Economics and Statistics*, 82, 1362–1374, https://doi.org/10.1111/obes.12369.

JERMANN, U. J. (1998): "Asset Pricing in Production Economies," *Journal of Monetary Economics*, 41, 257–275, https://doi.org/10.1016/S0304-3932(97)00078-0.

JURADO, K., S. C. LUDVIGSON, AND S. NG (2015): "Measuring Uncertainty," *American Economic Review*, 105, 1177–1216, https://www.doi.org/10.1257/aer.20131193.

JUSTINIANO, A. AND G. E. PRIMICERI (2008): "The Time-Varying Volatility of Macroeconomic Fluctuations," *American Economic Review*, 98, 604–41, https://www.doi.org/10.1257/aer.98.3.604.

KOOP, G., M. H. PESARAN, AND S. M. POTTER (1996): "Impulse Response Analysis in Nonlinear Multivariate Models," *Journal of Econometrics*, 74, 119–147, https://doi.org/10.1016/0304-4076(95)01753-4.

KOPECKY, K. AND R. SUEN (2010): "Finite State Markov-Chain Approximations to Highly Persistent Processes," *Review of Economic Dynamics*, 13, 701–714, https://doi.org/10.1016/j.red.2010.02.002.

LANNE, M. AND H. NYBERG (2016): "Generalized Forecast Error Variance Decomposition for Linear and Nonlinear Multivariate Models," *Oxford Bulletin of Economics and Statistics*, 78, 595–603, https://doi.org/10.1111/obes.12125.

LEDUC, S. AND Z. LIU (2016): "Uncertainty Shocks are Aggregate Demand Shocks," *Journal of Monetary Economics*, 82, 20–35, https://doi.org/10.1016/j.jmoneco.2016.07.002.

——— (2020): "The Weak Job Recovery in a Macro Model of Search and Recruiting Intensity," *American Economic Journal: Macroeconomics*, 12, 310–343, https://doi.org/10.1257/mac.20170176.

LJUNGQVIST, L. AND T. J. SARGENT (2017): "The Fundamental Surplus," *American Economic Review*, 107, 2630–2665, https://doi.org/10.1257/aer.20150233.

LUDVIGSON, S. C., S. MA, AND S. NG (2021): "Uncertainty and Business Cycles: Exogenous Impulse or Endogenous Response?" *American Economic Journal: Marcoeconomics*, 13, 369–410, https://www.doi.org/10.1257/mac.20190171.

MERZ, M. (1995): "Search in the Labor Market and the Real Business Cycle," *Journal of Monetary Economics*, 36, 269–300, https://doi.org/10.1016/0304-3932(95)01216-8.

MORTENSEN, D. AND E. NAGYPAL (2007): "More on Unemployment and Vacancy Fluctuations," *Review of Economic Dynamics*, 10, 327–347, https://doi.org/10.1016/j.red.2007.01.004.

MUMTAZ, H. AND F. ZANETTI (2013): "The Impact of the Volatility of Monetary Policy Shocks," *Journal of Money, Credit and Banking*, 45, 535–558, https://doi.org/10.1111/jmcb.12015.

NEWEY, W. K. AND K. D. WEST (1987): "A Simple, Positive Semi-Definite, Heteroskedasticity and Autocorrelation Consistent Covariance Matrix," *Econometrica*, 55, 703–708, https://www.doi.org/10.2307/1913610.

OH, J. (2020): "The Propagation of Uncertainty Shocks: Rotemberg versus Calvo," *International Economic Review*, 61, 1097–1113, https://doi.org/10.1111/iere.12450.

PETRONGOLO, B. AND C. A. PISSARIDES (2001): "Looking into the Black Box: A Survey of the Matching Function," *Journal of Economic Literature*, 39, 390–431, https://doi.org/10.1257/jel.39.2.390.

PETROSKY-NADEAU, N. AND L. ZHANG (2017): "Solving the Diamond-Mortensen-Pissarides model accurately," *Quantitative Economics*, 8, 611–650, https://doi.org/10.3982/QE452.

PETROSKY-NADEAU, N., L. ZHANG, AND L.-A. KUEHN (2018): "Endogenous Disasters," *American Economic Review*, 108, 2212–2245, https://doi.org/10.1257/aer.20130025.

PLANTE, M., A. W. RICHTER, AND N. A. THROCKMORTON (2018): "The Zero Lower Bound and Endogenous Uncertainty," *Economic Journal*, 128, 1730–1757, https://doi.org/10.1111/ecoj.12445.

RICHTER, A. W., N. A. THROCKMORTON, AND T. B. WALKER (2014): "Accuracy, Speed and Robustness of Policy Function Iteration," *Computational Economics*, 44, 445–476, https://doi.org/10.1007/s10614-013-9399-2.

ROTEMBERG, J. J. (1982): "Sticky Prices in the United States," *Journal of Political Economy*, 90, 1187–1211, https://doi.org/10.1086/261117.

ROUWENHORST, K. G. (1995): "Asset Pricing Implications of Equilibrium Business Cycle Models," in *Frontiers of Business Cycle Research*, ed. by T. F. Cooley, Princeton, NJ: Princeton University Press, 294–330.

RUGE-MURCIA, F. (2012): "Estimating Nonlinear DSGE Models by the Simulated Method of Moments: With an Application to Business Cycles," *Journal of Economic Dynamics and Control*, 36, 914–938, https://doi.org/10.1016/j.jedc.2012.01.008.

SAIJO, H. (2017): "The Uncertainty Multiplier and Business Cycles," *Journal of Economic Dynamics and Control*, 78, 1–25, https://doi.org/10.1016/j.jedc.2017.02.008.

SCHAAL, E. (2017): "Uncertainty and Unemployment," *Econometrica*, 85, 1675–1721, https://doi.org/10.3982/ECTA10557.

SEDLÁČEK, P. (2020): "Creative Destruction and Uncertainty," *Journal of the European Economic Association*, 18, 1814–1843, https://doi.org/10.1093/jeea/jvz047.

SHIMER, R. (2005): "The Cyclical Behavior of Equilibrium Unemployment and Vacancies," *American Economic Review*, 95, 25–49, https://doi.org/10.1257/0002828053828572.

——— (2012): "Reassessing the Ins and Outs of Unemployment," *Review of Economic Dynamics*, 15, 127–148, https://doi.org/10.1016/j.red.2012.02.001.

SIMS, C. A. (2002): "Solving Linear Rational Expectations Models," *Computational Economics*, 20, 1–20, https://doi.org/10.1023/A:1020517101123.

STRAUB, L. AND R. ULBRICHT (2015): "Endogenous Uncertainty and Credit Crunches," Toulouse School of Economics Working Paper 15-604.

——— (2019): "Endogenous second moments: A unified approach to fluctuations in risk, dispersion, and uncertainty," *Journal of Economic Theory*, 183, 625–660, https://doi.org/10.1016/j.jet.2019.07.007.

VAN NIEUWERBURGH, S. AND L. VELDKAMP (2006): "Learning Asymmetries in Real Business Cycles," *Journal of Monetary Economics*, 53, 753–772, https://doi.org/10.1016/j.jmoneco.2005.02.003.

A NASH BARGAINING

To derive the wage rate under Nash bargaining, define the total surplus of a new match as $\Lambda_t = \lambda_{n,t} + J_{N,t}^H - J_{U,t}^H$. $J_{N,t}^H$ and $J_{U,t}^H$ satisfy the employment and unemployment envelope conditions,

$$J_{N,t}^H = w_t + E_t[x_{t+1}((1 - \bar{s}(1 - \chi f_{t+1}))J_{N,t+1}^H + \bar{s}(1 - \chi f_{t+1})J_{U,t+1}^H)],$$
$$J_{U,t}^H = b + E_t[x_{t+1}(f_{t+1}J_{N,t+1}^H + (1 - f_{t+1})J_{U,t+1}^H)],$$

which are derived from the household's optimization problem given the following laws of motion:

$$n_{t+1} = (1 - \bar{s}(1 - \chi f_{t+1}))n_t + f_{t+1}u_t,$$
$$u_{t+1} = \bar{s}(1 - \chi f_{t+1})n_t + (1 - f_{t+1})u_t.$$

The equilibrium wage rate maximizes $(J_{N,t}^H - J_{U,t}^H)^\eta \lambda_{n,t}^{1-\eta}$, where $\eta \in [0, 1]$ is the household's bargaining weight. Optimality implies $J_{N,t}^H - J_{U,t}^H = \eta\Lambda_t$ and $\lambda_{n,t} = (1 - \eta)\Lambda_t$. After combining the optimality conditions with $J_{N,t}^H$, $J_{U,t}^H$, and (12), and defining tightness as $\theta_t = v_t/u_t^s$, we obtain

$$w_t = \eta((1 - \alpha)y_t/n_t + \kappa(1 - \chi\bar{s})E_t[x_{t+1}\theta_{t+1}]) + (1 - \eta)b.$$

The household's wage rate in period t is a weighted average of the firm's value of a new match and the worker's outside option b. The firm's value of a new worker includes the additional output produced plus the discounted expected value of the worker net of separations that occur in period $t+1$.

B EMPLOYMENT UNCERTAINTY DERIVATION

Under the assumptions in Section 4, the model collapses to

$$u_t^s = 1 - (1 - \chi\bar{s})n_{t-1}, \tag{20}$$
$$m_t = \xi(u_t^s)^\phi v_t^{1-\phi}, \tag{21}$$
$$n_t = (1 - \bar{s})n_{t-1} + m_t, \tag{22}$$
$$q_t = m_t/v_t, \tag{23}$$
$$\lambda_{n,t} = a_t - b + \beta(1 - \bar{s})E_t[\lambda_{n,t+1}], \tag{24}$$
$$\lambda_{n,t} = \kappa/q_t, \tag{25}$$
$$a_t = (1 - \rho_a)\bar{a} + \rho_a a_{t-1} + \sigma_{a,t-1}\varepsilon_{a,t}, \tag{26}$$
$$\sigma_{a,t} = (1 - \rho_{sv})\bar{\sigma}_a + \rho_{sv}\sigma_{a,t-1} + \sigma_{sv}\varepsilon_{sv,t}. \tag{27}$$

Note that the TFP processes are written in levels rather than logs to permit a closed-form solution.

Guess a solution of the form $\lambda_{n,t} = \delta_0 + \delta_1(a_t - \bar{a})$. Equating coefficients in (24) implies

$$\delta_0 = \frac{\bar{a} - b}{1 - \beta(1 - \bar{s})} > 0, \qquad \delta_1 = \frac{1}{1 - \beta(1 - \bar{s})\rho_a} > 0.$$

Therefore, match value uncertainty, $\sqrt{V_t[\lambda_{n,t+1}]} = \delta_1 \sigma_{a,t}$. From (21), (23), and (25), we obtain

$$q_t = \xi(u_t^s/v_t)^\phi = \kappa/\lambda_{n,t} \quad \rightarrow \quad v_t = u_t^s(\xi\lambda_{n,t}/\kappa)^{1/\phi}.$$

Therefore, the job finding rate is given by

$$f_t = m_t/u_t^s = q_t v_t/u_t^s = (\xi\lambda_{n,t}/\kappa)^{1/\phi}(\kappa/\lambda_{n,t}) = \xi^{1/\phi}(\lambda_{n,t}/\kappa)^{(1-\phi)/\phi}.$$

If we further assume $\phi = 0.5$, then uncertainty surrounding the job finding rate is given by

$$\sqrt{V_t[f_{n,t+1}]} = (\xi^2/\kappa)\delta_1\sigma_{a,t}.$$

From (22), employment uncertainty is then given by

$$\sqrt{V_t[\hat{n}_{t+1}]} = \frac{1}{n_t}u_{t+1}^s\sqrt{V_t[f_{t+1}]} = \frac{1}{n_t}u_{t+1}^s(\delta_1\xi^2/\kappa)\sigma_{a,t},$$

where the number of unemployed searching is predetermined according to (20).

C DATA SOURCES AND TRANSFORMATIONS

We use the following time-series from 1963-2019 provided by Haver Analytics:

1. **Civilian Noninstitutional Population: 16 Years & Over**
   Not Seasonally Adjusted, Quarterly, Thousands (LN16N@USECON)

2. **Gross Domestic Product: Implicit Price Deflator**
   Seasonally Adjusted, Quarterly, 2012=100 (DGDP@USNA)

3. **Gross Domestic Product**
   Seasonally Adjusted, Quarterly, Billions of Dollars (GDP@USECON)

4. **Personal Consumption Expenditures: Nondurable Goods**
   Seasonally Adjusted, Quarterly, Billions of Dollars (CN@USECON)

5. **Personal Consumption Expenditures: Services**
   Seasonally Adjusted, Quarterly, Billions of Dollars (CS@USECON)

6. **Personal Consumption Expenditures: Durable Goods**
   Seasonally Adjusted, Quarterly, Billions of Dollars (CD@USECON)

7. **Private Fixed Investment**

   Seasonally Adjusted, Quarterly, Billions of Dollars (F@USECON)

8. **Output Per Person**, Non-farm Business Sector, All Persons,

   Seasonally Adjusted, Quarterly, 2012=100 (LXNFS@USNA)

9. **Labor Share**, Non-farm Business Sector, All Persons,

   Seasonally Adjusted, Quarterly, Percent (LXNFBL@USNA)

10. **Unemployed, 16 Years & Over**

    Seasonally Adjusted, Monthly, Thousands (LTU@USECON)

11. **Civilian Labor Force: 16 yr & Over**

    Seasonally Adjusted, Monthly, Thousands (LF@USECON)

12. **Civilians Unemployed for Less Than 5 Weeks**

    Seasonally Adjusted, Monthly, Thousands (LU0@USECON)

13. **Job Openings**, Job Openings and Labor Turnover Survey,

    Seasonally Adjusted, Monthly, Thousands (LJJTLA@USECON)

14. **SPF Forecast Dispersion: Real GDP Growth**,

    Quarterly, 1-Quarter Ahead Growth Rate (ASAQ1GC@SURVEYS)

15. **CBOE Market Volatility Index: VIX**, Monthly, Index (SPVIX@USECON)

16. **Net Stock: Private Fixed Assets**, Annual, Billions of Dollars (EPT@CAPSTOCK)

17. **Net Stock: Durable Goods**, Annual, Billions of Dollars (EDT@CAPSTOCK)

18. **Depreciation: Private Fixed Assets**, Annual, Billions of Dollars (KPT@CAPSTOCK)

19. **Depreciation: Durable Goods**, Annual, Billions of Dollars (KDT@CAPSTOCK)

We also used the following data from other sources:

1. **Help Wanted Advertising Index (HWI)**, based on Barnichon (2010) and in units of the
   labor force. The series corrects for online advertising and is available on the author's website.

2. **Real Uncertainty (U)**, 3-month horizon, based on Ludvigson et al. (2021). The series is
   available on Ludvigson's website. The monthly series is averaged to a quarterly frequency.

We applied the following transformations to the above data sources:

1. **Per Capita Real Output**: $Y_t = GDP_t/(DGDP_t \times LN16N_t)$.

2. **Per Capita Real Consumption**: $C_t = (CN_t + CS_t)/(DGDP_t \times LN16N_t)$.

3. **Per Capita Real Investment**: $I_t = (F_t + CD_t)/(DGDP_t \times LN16N_t)$.

4. **Unemployment Rate**: $U_t = 100(LTU_t/LF_t)$.

5. **Vacancy Rate**: HWI from 1963M1-2000M12 and $LJJTLA/LF$ from 2001M1-2019M12.

6. **Short-term Unemployed** (U^s): The redesign of the Current Population Survey (CPS) in 1994 reduced u_t^s. To correct for this bias, we follow Elsby et al. (2009) and scale u_t^s by the time average of the ratio of u_t^s/u_t for the first and fifth rotations groups to u_t^s/u_t across all rotation groups. Using IPUMS-CPS data, we extract EMPSTAT ("Employment Status"), DURUNEMP ("Continuous weeks unemployed") and MISH ("Month in sample, household level"). Unemployed persons have EMPSTAT equal to 20, 21, or 22. Short-term unemployed are persons who are unemployed and have DURUNEMP equal to 4 or less. Incoming rotation groups have MISH equal to 1 or 5. Using the final weights, WTFINL, we calculate unemployment rates conditional on the appropriate values of MISH and DURUNEMP. We then apply the X-12 seasonal adjustment function in STATA to the time series for the ratio. Finally, we take an average of the seasonally adjusted series from 1994-2019. This process yields an average of 1.1725, so U^s equals $LU0$ prior to 1994 and $1.1725 \times LU0$ after 1994.

7. **Job-Finding Rate**: Following Shimer (2005), $f_t = 1 - (LTU_{t+1} - U_{t+1}^s)/LTU_t$.

8. **Job Separation Rate**: Following Shimer (2012), $s_t = 1 - \exp(-\tilde{s}_t)$, where $\tilde{s}_t$ satisfies

$$LTU_{t+1} = \frac{(1 - \exp(-\tilde{f}_t - \tilde{s}_t))\tilde{s}_t LF_t}{\tilde{f}_t + \tilde{s}_t} + \exp(-\tilde{f}_t - \tilde{s}_t)LTU_t, \quad \tilde{f}_t = -\log(1 - f_t).$$

9. **Real Wage**: Following Hagedorn and Manovskii (2008), $w_t = LXNFBL_t \times LXNFS_t$.

10. **Wage Elasticity**: Slope coefficient from regressing w_t on an intercept and $LXNFS_t$.

11. **Depreciation Rate**: $\delta = (1 + \frac{1}{T/12} \sum_{t=1}^{T/12} (KPT_t + KDT_t)/(EPT_{t-1} + EDT_{t-1}))^{1/12} - 1$.

12. **Capital Share of Income**: $\alpha = 1 - \frac{1}{T/3} \sum_{t=1}^{T/3} LXNFBL$.

13. **Inflation Rate**: $\bar{\pi} = \frac{1}{T/3} \sum_{t=1}^{T/3} (1 + \log(DGDP_t/DGDP_{t-1}))^{1/3}$.

All monthly time series are averaged to a quarterly frequency. The data is detrended using a Hamilton filter with an 8 quarter window. All empirical targets are computed using quarterly data.

D SOLUTION METHOD

The equilibrium system of the model is summarized by $E[g(\mathbf{x}_{t+1}, \mathbf{x}_t, \varepsilon_{t+1})|\mathbf{z}_t, \vartheta] = 0$, where g is a vector-valued function, $\mathbf{x}_t$ is a vector of variables, ε_t is a vector of shocks, $\mathbf{z}_t$ is a vector of states, and ϑ is a vector of parameters. There are many ways to discretize the TFP level shock and volatility process. We use the Markov chain in Rouwenhorst (1995), which Kopecky and Suen (2010) show outperforms other methods for approximating autoregressive processes. For our estimated

model, the bounds on a_t and k_{t-1} are set to $\pm 8\%$ of their deterministic steady states, while n_{t-1} ranges from 0.88 to 0.98. These bounds ensure that simulations contain at least 99% of the ergodic distribution. We specify 9 states for $\sigma_{a,t}$, 9 states for $\varepsilon_{a,t+1}$, and discretize a_t, k_{t-1}, and n_{t-1} into 13, 9, and 9 evenly-spaced points, respectively.[18] The product of the points in each dimension, D, is the total nodes in the state space ($D = 9{,}477$). The realization of $\mathbf{z}_t$ on node d is denoted $\mathbf{z}_t(d)$. The Rouwenhorst method provides integration nodes, $[\varepsilon_{a,t+1}(m), \sigma_{a,t+1}(m)]$, with weights, $\phi(m)$, for $m \in \{1, \ldots, M\}$. The realizations of $\sigma_{a,t+1}$ are the same as $\sigma_{a,t}$ because it is a Markov chain.

Since vacancies $v_t \geq 0$, we introduce an auxiliary variable, μ_t, such that $v_t = \max\{0, \mu_t\}^2$ and $\lambda_t = \max\{0, -\mu_t\}^2$, where λ_t is the Lagrange multiplier on the non-negativity constraint. If $\mu_t \geq 0$, then $v_t = \mu_t^2$ and $\lambda_t = 0$. When $\mu_t < 0$, the constraint is binding, $v_t = 0$, and $\lambda_t = \mu_t^2$. Therefore, the constraint on v_t is transformed into a pair of equalities (Garcia and Zangwill, 1981).

The vector of policy functions and the realization on node d are denoted by $\mathbf{pf}_t$ and $\mathbf{pf}_t(d)$, where $\mathbf{pf}_t \equiv [\mu_{v,t}(\mathbf{z}_t), c_t(\mathbf{z}_t)]$. The following steps outline our policy function iteration algorithm:

1. Use Sims's (2002) `gensys` algorithm to solve the log-linear model. Then map the solution for the policy functions to the discretized state space. This provides an initial conjecture.

2. On iteration $j \in \{1, 2, \ldots\}$ and each node $d \in \{1, \ldots, D\}$, use Chris Sims's `csolve` to find $\mathbf{pf}_t(d)$ to satisfy $E[g(\cdot)|\mathbf{z}_t(d), \vartheta] \approx 0$. Guess $\mathbf{pf}_t(d) = \mathbf{pf}_{j-1}(d)$. Then apply the following:

   (a) Solve for all variables dated at time t, given $\mathbf{pf}_t(d)$ and $\mathbf{z}_t(d)$.

   (b) Linearly interpolate the policy functions, $\mathbf{pf}_{j-1}$, at the updated state variables, $\mathbf{z}_{t+1}(m)$, to obtain $\mathbf{pf}_{t+1}(m)$ on every integration node, $m \in \{1, \ldots, M\}$.

   (c) Given $\{\mathbf{pf}_{t+1}(m)\}_{m=1}^M$, solve for the other elements of $\mathbf{s}_{t+1}(m)$ and compute

   $$E[g(\mathbf{x}_{t+1}, \mathbf{x}_t(d), \varepsilon_{t+1})|\mathbf{z}_t(d), \vartheta] \approx \sum_{m=1}^M \phi(m) g(\mathbf{x}_{t+1}(m), \mathbf{x}_t(d), \varepsilon_{t+1}(m)).$$

   When `csolve` converges, set $\mathbf{pf}_j(d) = \mathbf{pf}_t(d)$.

3. Repeat step 2 until $\mathrm{maxdist}_j < 10^{-6}$, where $\mathrm{maxdist}_j \equiv \max\{|\mathbf{pf}_j - \mathbf{pf}_{j-1}|\}$. When that criterion is satisfied, the algorithm has converged to an approximate nonlinear solution.

The algorithm is programmed in Fortran with Open MPI and run on the BigTex supercomputer.

E ESTIMATION METHOD

The estimation procedure has two stages. The first stage estimates moments in the data using a 2-step Generalized Method of Moments (GMM) estimator with a Newey and West (1987) weighting matrix with 5 lags. The second stage is a Simulated Method of Moments (SMM) procedure that

---

[18] We also tried using a grid that was more than 10 times denser, but it had very little effect on our quantitative results.

searches for a parameter vector that minimizes the distance between the GMM estimates in the data and short-sample predictions of the model, weighted by the diagonal of the GMM estimate of the variance-covariance matrix. The second stage is repeated for many different draws of shocks to obtain the standard errors on the parameter estimates. The following steps outline the algorithm:

1. Use GMM to estimate the targets, $\hat{\Psi}_T^D$, and the diagonal of the covariance matrix, $\hat{\Sigma}_T^D$.

2. Use SMM to estimate the nonlinear DMP model. Given a random seed, h, draw a $B + T$ period sequence for each shock in the model, where $B = 1{,}000$ is a burn-in period and $T = 687$ is the length of the monthly time series. Denote the shock matrix by $\mathcal{E}^s = [\varepsilon_a^s, \varepsilon_{sv}^s]_{t=1}^{B+T})$.

   For shock sequence $s \in \{1, \ldots, N_s\}$, run the following steps:

   (a) Evaluate the loss function for $i \in \{1, \ldots, N_m\}$ random draws in the parameter space.

      i. Draw a vector of parameters $\hat{\mathcal{P}}_i$ from a multivariate normal distribution centered at a specified mean parameter vector, $\bar{\mathcal{P}}$, with diagonal covariance matrix, Σ_0.

      ii. Solve the model using the algorithm in Appendix D given $\hat{\mathcal{P}}_i$. Return to step i if the linear solution does not exist or the nonlinear algorithm does not converge.

      iii. Given $\mathcal{E}^s(r)$, simulate the model R times for $B + T$ periods. We draw initial states from the ergodic distribution by burning off the first B periods and aggregate to a quarterly frequency. For each repetition r, calculate the moments $\Psi_T^M(\hat{\mathcal{P}}_i, \mathcal{E}^s(r))$.

      iv. Calculate the mean moments $\bar{\Psi}_{R,T}^M(\hat{\mathcal{P}}_i, \mathcal{E}^s) = \frac{1}{R} \sum_{r=1}^{R} \Psi_T^M(\hat{\mathcal{P}}_i, \mathcal{E}^s(r))$ and the fit

      $$J_i = [\hat{\Psi}_T^D - \bar{\Psi}_{R,T}^M(\hat{\mathcal{P}}_i, \mathcal{E}^s)]'[\hat{\Sigma}_T^D(1 + 1/R)]^{-1}[\hat{\Psi}_T^D - \bar{\Psi}_{R,T}^M(\hat{\mathcal{P}}_i, \mathcal{E}^s)].$$

   (b) Find a guess, $\hat{\mathcal{P}}_0$, for the N_p estimated parameters and the covariance matrix, Σ_0:

      i. Find the parameter draw $\hat{\mathcal{P}}_0$ that corresponds to $\min\{J_i\}_{i=1}^{N_m}$.

      ii. Find all J_i below the median, stack the corresponding draws in a $N_m/2 \times N_p$ matrix, $\hat{\Theta}$, and define the (i,j) element as $\tilde{\Theta}_{i,j} = \hat{\Theta}_{i,j} - \sum_{i=1}^{N_m/2} \hat{\Theta}_{i,j}/(N_m/2)$.

      iii. Calculate $\Sigma_0 = \tilde{\Theta}'\tilde{\Theta}/(N_m/2)$.

   (c) Minimize J with simulated annealing. For $i \in \{0, \ldots, N_d\}$, repeat the following steps:

      i. Draw a candidate vector of parameters, $\hat{\mathcal{P}}_i^{cand}$, where

      $$\hat{\mathcal{P}}_i^{cand} \sim \begin{cases} \hat{\mathcal{P}}_0 & \text{for } i = 0, \\ \mathbb{N}(\hat{\mathcal{P}}_{i-1}, c_0\Sigma_0) & \text{for } i > 0. \end{cases}$$

      We set c_0 to target an average acceptance rate of 50% across seeds.

      ii. Repeat steps 2a, ii-iv.

33

iii. Accept or reject the candidate draw according to

$$(\hat{\mathcal{P}}_i, J_i) = \begin{cases} (\hat{\mathcal{P}}_i^{cand}, J_i^{cand}) & \text{if } i = 0, \\ (\hat{\mathcal{P}}_i^{cand}, J_i^{cand}) & \text{if } \min(1, \exp(J_{i-1} - J_i^{cand})/c_1) > \hat{u}, \\ (\hat{\mathcal{P}}_{i-1}, J_{i-1}) & \text{otherwise,} \end{cases}$$

where c_1 is the temperature and $\hat{u}$ is a draw from a uniform distribution.

(d) Find $\hat{\mathcal{P}}_0^{up}$ and Σ_0^{up} following step 2b.

(e) Repeat steps 2c-d N_{SMM} times, initializing at $\hat{\mathcal{P}}_0 = \hat{\mathcal{P}}_0^{up}$ and $\Sigma_0 = \Sigma_0^{up}$. Gradually decrease the temperature. Across all N_{SMM} stages, find the lowest J value, denoted J^{guess}, and the corresponding draw, $\mathcal{P}^{guess}$.

(f) Minimize the same loss function with MATLAB's `fminsearch` starting at $\mathcal{P}^{guess}$. The minimum is $\hat{\mathcal{P}}^{\min}$ with a loss function value of $J^{\min}$. Repeat, each time updating the guess, until $J^{guess} - J^{\min} < 0.001$. The parameter estimates correspond to $J^{\min}$.

Given $\{\hat{\mathcal{P}}^s\}_{s=1}^{N_s}$, we report the mean, $\bar{\mathcal{P}} = \sum_{s=1}^{N_s} \hat{\mathcal{P}}^s / N_s$ and standard errors of the estimates. The reported moments are then based on the mean parameter estimates, $\bar{\Psi}_T^M = \bar{\Psi}_{R,T}^M(\bar{\mathcal{P}}, \mathcal{E})$.

We set $N_s = 200$, $R = 1,000$, $N_{SMM} = 3$, $N_m = 1,000$, $N_d = 500$, and $N_p = 10$. For each simulated annealing stage, c_0 is 0.1, 0.7, and 1.0, and c_1 is 1.0, 0.5, and 0.25, respectively. The algorithm was programmed in Fortran and executed with Open MPI on the BigTex supercomputer.

F HOME PRODUCTION

This section shows our results are robust to alternative sources of unemployment volatility. To demonstrate this, we extend our baseline model to include home production following Petrosky-Nadeau et al. (2018). The representative household derives utility from the consumption of both the final market good $c_{m,t}$ and home production $c_{h,t}$. It has log utility over composite consumption $c_t = (\omega c_{m,t}^e + (1 - \omega) c_{h,t}^e)^{1/e}$, where $\omega \in (0, 1)$ is the preference weight on the market good and $e \leq 1$ governs the elasticity of substitution $1/(1 - e)$. The home production technology is $c_{h,t} = a_h u_t$, where $a_h > 0$ is productivity. The rest of the model is identical to the baseline model.

Household optimization yields the pricing kernel $x_{t+1} = \beta(c_{m,t}/c_{m,t+1})^{1-e}(c_t/c_{t+1})^e$. The flow value of unemployment becomes $z_t = a_h((1 - \omega)/\omega)(c_{m,t}/c_{h,t})^{1-e} + b$, so the Nash wage satisfies

$$w_t = \eta((1 - \alpha)y_t/n_t + \kappa(1 - \chi\bar{s})E_t[x_{t+1}\theta_{t+1}]) + (1 - \eta)z_t.$$

The remaining equilibrium conditions are unchanged from the baseline model shown in Section 3.

We set $b = 0.4$ to reflect the value of unemployment benefits (Shimer, 2005). The remaining baseline parameters are set to their estimated values shown in Table 2a. We set a_h to the steady-

state marginal product of labor in final good production. We then calibrate $\omega = 0.7$ and $e = 0.9$ to target the standard deviations of unemployment and final good output in the baseline DMP model.

Moment	Baseline	Home Production
$SD(\mathcal{U})$	6.06	5.84
$SD(\tilde{y})$	3.65	3.64
$SD(\tilde{u})$	21.14	21.29
$Corr(\mathcal{U}, \tilde{y})$	−0.62	−0.59

Table 9: Key Moments

Contribution	Output	Uncertainty
Level Total	100.00	36.72
Volatility Total	0.19	63.50
Level Direct	99.81	36.50
Volatility Direct	0.00	63.28

Table 10: Home production variance decomposition

Results Table 9 compares the moments from the home production model to the baseline model and Table 10 shows the variance decomposition. The model continues to generate a strong negative correlation between output and uncertainty and similar business cycle moments. Level shocks continue to explain almost all of the output variance and about 40% of the uncertainty variance. Crucially, these results stem from a much lower value of b that only reflects unemployment benefits, as in Shimer (2005). This shows our mechanism is robust to other sources of labor market volatility.

G EFFECT OF CAPITAL ADJUSTMENT COSTS

Given the importance of the employment law of motion, this section studies the effect of adjustment costs in the capital law of motion using textbook Real Business Cycle and New Keynesian models.

G.1 REAL BUSINESS CYCLE MODEL

A representative household chooses $\{c_t, n_t, k_t\}_{t=0}^{\infty}$ to maximize expected lifetime utility, $E_0 \sum_{t=0}^{\infty} \beta^t [\ln c_t - \vartheta \frac{n_t^{1+\gamma}}{1+\gamma}]$, where ϑ determines steady-state labor hours and $1/\gamma$ is the Frisch elasticity of labor supply. The household's choices are constrained by $c_t + i_t = w_t n_t + r_t^k k_{t-1}$ and the law of motion for capital in (9). Optimality implies (10) and

$$w_t = \vartheta n_t^\gamma c_t. \tag{28}$$

The representative firm produces output with the following technology,

$$y_t = a_t k_{t-1}^\alpha n_t^{1-\alpha}, \tag{29}$$

where α is the capital share of income. The firm chooses $\{n_t, k_{t-1}\}$ to maximize current profits, $y_t - w_t n_t - r_t^k k_{t-1}$, subject to the production function. The two optimality conditions are given by

$$w_t = (1 - \alpha) y_t / n_t, \tag{30}$$

$$r_t^k = \alpha y_t / k_{t-1}. \tag{31}$$

The aggregate resource constraint is given by

$$c_t + i_t = y_t. \tag{32}$$

A competitive equilibrium consists of infinite sequences of quantities $\{y_t, k_t, c_t, n_t, i_t\}_{t=0}^{\infty}$, prices $\{w_t, r_t^k\}_{t=0}^{\infty}$, and exogenous variables $\{a_t, \sigma_{a,t}\}_{t=0}^{\infty}$ that satisfy (1), (2), (9), (10), and (28)-(32), given the state of the economy $\{k_{-1}, a_{-1}, \sigma_{a,-1}\}$ and the sequences of TFP shocks $\{\varepsilon_{a,t}, \varepsilon_{\sigma_a,t}\}_{t=1}^{\infty}$.

G.2 NEW KEYNESIAN MODEL

The production sector now consists of a continuum of monopolistically competitive intermediate firms and a representative final good firm. Intermediate firm $f \in [0,1]$ produces a differentiated good, $y_{f,t} = a_t k_{f,t-1}^{\alpha} n_{f,t}^{1-\alpha}$, where n_{f_t} and $k_{f,t-1}$ are the labor and capital inputs used by firm f. The final good firm purchases output from each intermediate firm to produce the final good, $y_t \equiv [\int_0^1 y_{f,t}^{(\theta-1)/\theta} df]^{\theta/(\theta-1)}$, where $\theta > 1$ is the elasticity of substitution.

Profit maximization by the final good firm determines the demand for intermediate good f, $y_{f,t} = (p_{f,t}/p_t)^{-\theta} y_t$, where $p_t = [\int_0^1 p_{f,t}^{1-\theta} df]^{1/(1-\theta)}$ is the price level. Following Rotemberg (1982), intermediate firms pay a price adjustment cost, $\Lambda_{f,t}^p \equiv \varphi(p_{f,t}/(\bar{\pi} p_{f,t-1}) - 1)^2 y_t/2$, where $\varphi > 0$ scales the cost and $\bar{\pi}$ is the steady-state inflation rate. Given this cost, the value of firm f satisfies

$$V_{f,t} = \max_{n_{f,t}, k_{f,t-1}, p_{f,t}} p_{f,t} y_{f,t}/p_t - w_t n_{f,t} - r_t^k k_{f,t-1} - \Lambda_{f,t}^p + E_t[x_{t+1} V_{f,t+1}],$$

subject to $y_{f,t} = a_t k_{f,t-1}^{\alpha} n_{f,t}^{1-\alpha}$ and $y_{f,t} = (p_{f,t}/p_t)^{-\theta} y_t$. In a symmetric equilibrium where $p_{f,t} = p_t$, optimality implies the input demand schedules and New Keynesian Phillips curve are given by

$$w_t = (1-\alpha) mc_t y_t/n_t, \tag{33}$$

$$r_t^k = \alpha mc_t y_t/k_{t-1}, \tag{34}$$

$$\varphi(\pi_t/\bar{\pi} - 1)(\pi_t/\bar{\pi}) = 1 - \theta + \theta mc_t + \varphi E_t[x_{t+1}(\pi_{t+1}/\bar{\pi} - 1)(\pi_{t+1}/\bar{\pi}) y_{t+1}/y_t], \tag{35}$$

where $\pi_t = p_t/p_{t-1}$ is the gross inflation rate. If $\varphi = 0$, then the real marginal cost of producing a unit of output, mc_t, equals $(\theta-1)/\theta$, which is the inverse of the markup of price over marginal cost.

In addition to capital, the household has access to a one-period nominal bond, so the budget constraint is $c_t + i_t + b_t = w_t n_t + r_t^k k_{t-1} + r_{t-1} b_{t-1}/\pi_t + d_t$, where r_t is the gross nominal interest rate and d_t is dividends from ownership of firms. The optimality conditions imply (10), (28), and

$$1 = E_t[x_{t+1}(r_t/\pi_{t+1})]. \tag{36}$$

The bond is in zero net supply and the central bank sets the nominal interest rate according to

$$r_t = \bar{r}(\pi_t/\bar{\pi})^{\phi_\pi}, \tag{37}$$

where $\bar{r}$ is the nominal interest rate target and ϕ_π governs the strength of the response to inflation.

A competitive equilibrium consists of infinite sequences of quantities $\{y_t, k_t, c_t, n_t, i_t, mc_t\}_{t=0}^\infty$, prices $\{w_t, r_t^k, r_t, \pi_t\}_{t=0}^\infty$, and exogenous variables $\{a_t, \sigma_{a,t}\}_{t=0}^\infty$ that satisfy (1), (2), (9), (10), (28), (29), and (32)-(37), given the initial state $\{k_{-1}, a_{-1}, \sigma_{a,-1}\}$ and sequences of shocks $\{\varepsilon_{a,t}, \varepsilon_{\sigma_a,t}\}_{t=1}^\infty$.

Parameter	RBC	NK	Calibration Target
Frisch Elasticity ($1/\gamma$)	0.5	0.5	Chetty et al. (2012)
Capital Adjustment Cost (ν)	20	20	Investment Standard Deviation
Elasticity of Substitution (θ)	−	11	10% Price Markup
Monetary Response to Inflation (ϕ_π)	−	1.5	Leduc and Liu (2016)
Price Adjustment Costs (φ)	−	1,296	Leduc and Liu (2016)
Steady-State Hours ($\bar{n}$)	0.33	0.33	Standard Value
Steady-State Inflation Rate ($\bar{\pi}$)	−	1.0028	Average Inflation Rate
Level Shock Persistence (ρ_a)	0.95	0.95	Output Autocorrelation
Volatility Shock Persistence (ρ_{sv})	0.87	0.87	Leduc and Liu (2016)
Level Shock SD ($\bar{\sigma}_a$)	0.0079	0.0078	Output Standard Deviation
Volatility Shock SD (σ_{sv})	0.0357	0.0354	Uncertainty Standard Deviation

Table 11: Real Business Cycle and New Keynesian model calibrations.

G.3 CALIBRATION   Both models are calibrated at a monthly frequency. Table 11 summarizes the parameter values. We set the level shock persistence (ρ_a) and standard deviation ($\bar{\sigma}_a$) to match the autocorrelation and volatility of detrended output. We calibrate the volatility shock standard deviation (σ_{sv}) to match the volatility of real uncertainty and the capital adjustment cost parameter (ν) to target the volatility of investment. Other parameters are calibrated in line with the literature.

Moment	Data	Model RBC	Model NK
$SD(\mathcal{U})$	5.93	5.93	5.93
$SD(\tilde{y})$	3.15	3.15	3.15
$SD(\tilde{\imath})$	8.68	7.36	7.80
$Corr(\mathcal{U}, \tilde{y})$	−0.60	0.01	0.11

Table 12: Key Moments

Contribution	Output RBC	Output NK	Uncertainty RBC	Uncertainty NK
Level Total	100.00	100.00	0.03	1.43
Volatility Total	0.38	0.37	99.97	98.58
Level Direct	99.62	99.63	0.03	1.42
Volatility Direct	0.00	0.00	99.97	98.57

Table 13: Variance decompositions

G.4 RESULTS   Table 12 shows that neither model generates countercyclical uncertainty, as the correlation between output and uncertainty is slightly positive in both models. This holds even though both models match the volatility of uncertainty and generate realistic investment dynamics. Thus, capital adjustment costs are too weak to generate endogenous fluctuations in uncertainty. Instead, Table 13 shows uncertainty dynamics are mostly driven by the exogenous volatility shocks.

H HOSIOS CONDITION

The equilibrium of a search and matching model is generally inefficient due to two externalities in the matching process (Hosios, 1990). First, when a firm posts a new vacancy, it imposes a positive externality on unemployed workers who face a higher job finding rate. Second, the vacancy posting imposes a negative externality on other firms who face lower job filling rates and a higher marginal cost of vacancy creation today and in the future. The Hosios (1990) condition restores efficiency.

Social Planner Problem The social planner maximizes

$$W_t = \ln c_t + \beta E_t W_{t+1}$$

subject to

$$c_t \leq a_t k_{t-1}^\alpha n_t^{1-\alpha} - \kappa v_t - i_t + b u_t - \tau_t,$$

$$n_t \leq (1-s)n_{t-1} + \xi(1 - n_{t-1} + \chi \bar{s} n_{t-1})^\phi v_t^{1-\phi},$$

$$k_t \leq (1-\delta)k_{t-1} + \left(a_1 + \frac{a_2}{1 - 1/\nu}\left(\frac{i_t}{k_{t-1}}\right)^{1-1/\nu}\right)k_{t-1},$$

$$u_t = 1 - n_t, \quad v_t \geq 0.$$

The optimality conditions for job creation and investment are given by

$$\frac{\kappa - \lambda_{v,t}}{(1-\phi)q_t} = (1-\alpha)\frac{y_t}{n_t} - b + E_t\left[x_{t+1}\left(\frac{\kappa - \lambda_{v,t+1}}{(1-\phi)q_{t+1}}\right)(1 - s - \phi(1-\chi\bar{s})f_{t+1})\right], \quad (38)$$

$$\frac{1}{a_2}\left(\frac{i_t}{k_{t-1}}\right)^{1/\nu} = E_t\left[x_{t+1}\left(\alpha\frac{y_{t+1}}{k_t} + \frac{1}{a_2}\left(\frac{i_{t+1}}{k_t}\right)^{1/\nu}(1-\delta+a_1) + \frac{1}{\nu-1}\frac{i_{t+1}}{k_t}\right)\right], \quad (39)$$

where $\lambda_{v,t}$ is the multiplier on the non-negativity constraint for v_t, and $x_{t+1} \equiv \beta(c_t/c_{t+1})$.

Competitive Equilibrium In competitive equilibrium, the job creation condition is given by

$$\frac{\kappa - \lambda_{v,t}}{q_t} = (1-\alpha)y_t/n_t - w_t + (1-\bar{s})E_t\left[x_{t+1}\frac{\kappa - \lambda_{v,t+1}}{q_{t+1}}\right], \quad (40)$$

while (39) is unchanged. The wage rule resulting from Nash bargaining is given by

$$w_t = \eta((1-\alpha)y_t/n_t + \kappa(1-\chi\bar{s})E_t[x_{t+1}\theta_{t+1}]) + (1-\eta)b. \quad (41)$$

Note that labor market tightness is $\theta_t = v_t/u_{t-1} = f_t/q_t$. Combine (40) and (41) to obtain

$$\frac{\kappa - \lambda_{v,t}}{q_t} = (1-\eta)\left((1-\alpha)\frac{y_t}{n_t} - b\right) + E_t\left[x_{t+1}\left(\frac{\kappa - \lambda_{v,t+1}}{q_{t+1}}\right)\left(1 - \bar{s} - \eta\kappa(1-\chi\bar{s})\frac{f_{t+1}}{\kappa - \lambda_{v,t+1}}\right)\right] \quad (42)$$

Hosios Condition If $v_{t+1} > 0$, then $\lambda_{v,t+1} = 0$. If $v_{t+1} = 0$, then $m_{t+1} = f_{t+1} = 0$. In either case, (42) is equivalent to (38) when the Nash bargaining weight equals the matching elasticity, $\eta = \phi$.

I VAR ESTIMATES UNDER RECURSIVE IDENTIFICATION

Recursive identification schemes are often used to identify the effect of uncertainty shocks on real activity. To show the implications of our theoretical results, consider the following bivariate VAR,

$$Y_t = \sum_{l=1}^{L} A_l Y_{t-l} + v_t, \tag{43}$$

where Y_t is a vector of output and uncertainty, v_t is a vector of reduced-form shocks, and $\{A_l\}_{l=1}^{L}$ are parameter matrices. Suppose uncertainty is ordered first in Y_t and a Cholesky decomposition is used to identify the structural shocks. Under these assumptions, uncertainty shocks can affect uncertainty and output on impact, while output shocks can only affect output contemporaneously.

To test whether this recursive identification scheme can identify the true structural output responses, we estimate the VAR model on quarterly actual and simulated data from our estimated DMP model and compare the identified responses. The number of lags $L = 3$ is based on the Akaike Information Criterion. We simulate our model $1,000$ times to produce artificial data series with 228 quarterly (684 monthly) observations, the same number used for our structural estimation.

Figure 3 reports the responses to an uncertainty shock using actual and simulated data at a quarterly frequency under a recursive identification scheme. The responses with actual data are similar to those in the literature: a positive uncertainty shock raises uncertainty and lowers output on impact. We obtain similar responses using our simulated data VAR even though the model violates the identification assumption. Only the level shock affects output on impact in the simulated data, so the identified "structural" shock must be correlated with the level shock from the DMP model. We confirm this intuition by estimating the VAR model on simulated *monthly* data (i.e., the frequency of the model) and correlating the identified structural shocks with the true structural shocks. While the identified uncertainty shock has a correlation of 0.88 with the true structural uncertainty shock, it also has a correlation of -0.47 with the true structural level shock, confirming it is contaminated.

Alternatively, when uncertainty is ordered last in the VAR, the identified output shock has a correlation of 0.99 with the true level shock and 0 with the true uncertainty shock. The identified uncertainty shock has a correlation of 0.96 with the true uncertainty shock and 0 with the level shock. These correlations show the recursive identification scheme properly identifies the structural shocks under this ordering because uncertainty is almost entirely endogenous in the DMP model. Figure 4 shows the impulse responses to an uncertainty shock using actual and simulated data in this case. Consistent with the impulse responses from the DMP model, there is almost no real effect of uncertainty using the simulated data VAR. Using actual data, the real effects are smaller than when uncertainty is ordered first, but there is still a statistically significant decline in output. One potential explanation is that uncertainty in the data has meaningful endogenous *and* exogenous components. In this setting, neither recursive ordering will properly identify the structural shocks.
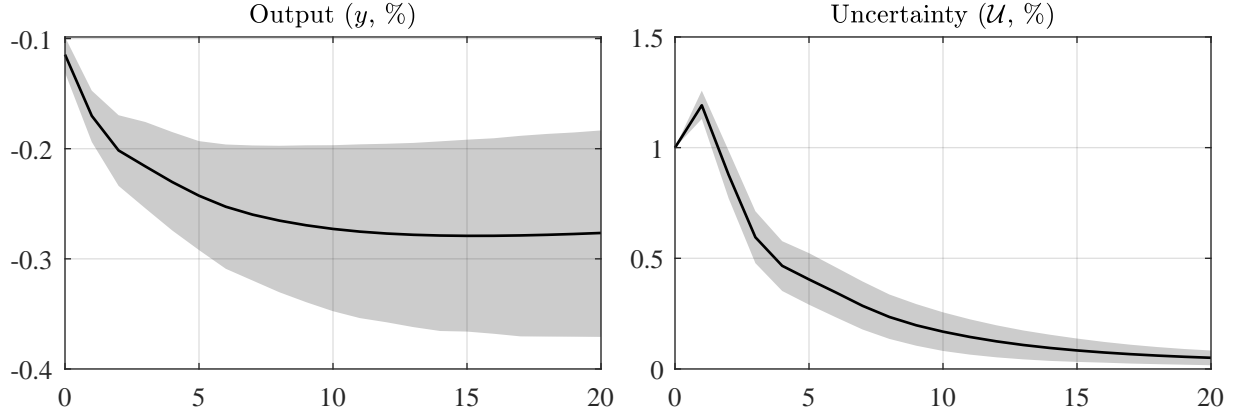
(a) Responses based on actual data. Shaded regions are 68% confidence intervals.
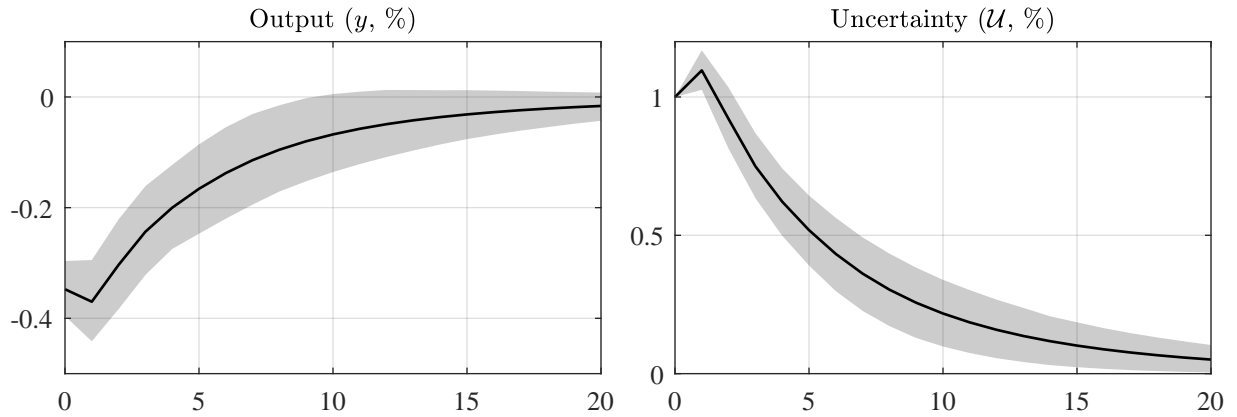
(b) Responses based on simulated data. Shaded regions are $[16\%, 84\%]$ credible sets.

Figure 3: Bivariate VAR responses to an uncertainty shock when uncertainty is ordered first.

J   VARIABLE SEARCH INTENSITY MODEL

This section shows our results are robust to adding search effort to the baseline DMP model following Leduc and Liu (2020). Define z_t as average search intensity, so new matches are given by

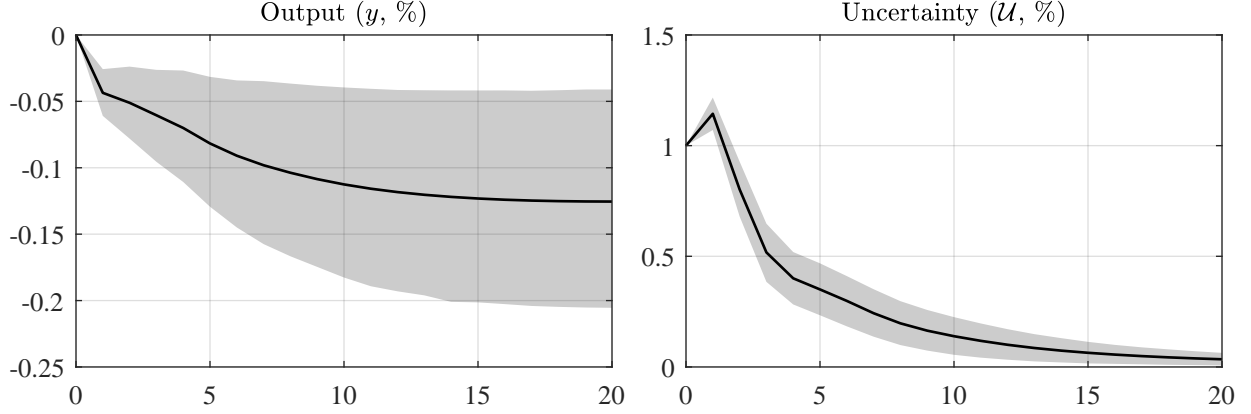$$\mathcal{M}_t = \xi(z_t u_t^s)^\phi v_t^{1-\phi}.$$

The household chooses consumption, investment, capital, and search intensity to solve

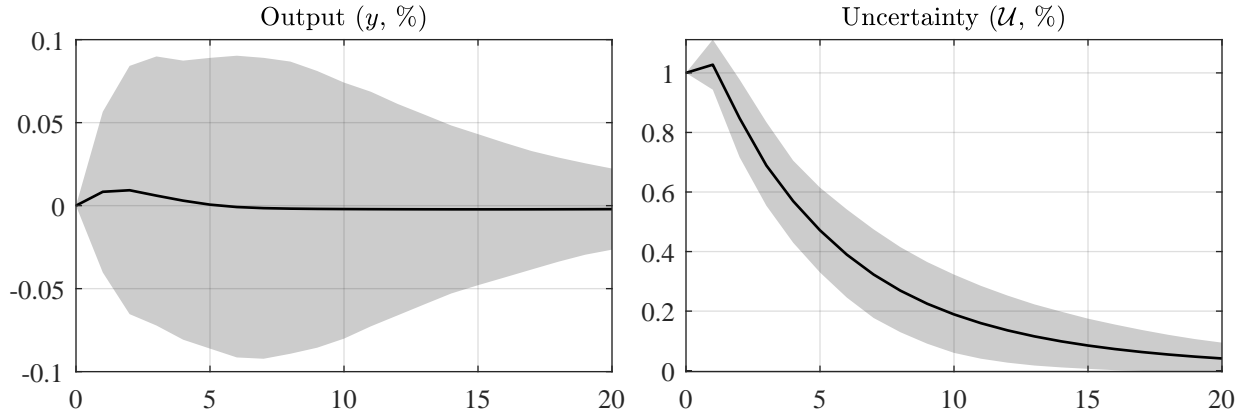$$J_t^H = \max_{c_t, i_t, k_t, z_t} \ln c_t + \beta E_t[J_{t+1}^H]$$

subject to (6), (9), and

$$c_t + i_t = w_t n_t + r_t^k k_{t-1} + b(1 - n_t) - h(z_t)u_t^s - \tau_t,$$

where $h(z_t)$ is the resource cost of search effort, which is increasing and concave. For a worker

(a) Responses based on actual data. Shaded regions are 68% confidence intervals.

(b) Responses based on simulated data. Shaded regions are $[16\%, 84\%]$ credible sets.

Figure 4: Bivariate VAR responses to an uncertainty shock when uncertainty is ordered last.

with search effort z_{it}, the job finding rate is $f(z_{it}) = z_{it}m_t/(s_t u_t^s)$, so the marginal effect of raising search intensity is $\partial f(z_{it})/\partial z_{it} = f_t/z_t$. The optimality and envelope conditions produce (10) and

$$h'(z_t) = \frac{f_t}{z_t}\left(w_t - b + E_t\left[x_{t+1}(1 - f_{t+1} - \bar{s}(1 - \chi f_{t+1}))\tilde{J}_{n,t+1}\right]\right), \qquad (44)$$

$$\tilde{J}_{n,t} = w_t - b + E_t[x_{t+1}(1 - f_{t+1} - \bar{s}(1 - \chi f_{t+1}))\tilde{J}_{n,t+1}] + h(z_t)\frac{1 - \chi\bar{s}}{1 - f_t - \bar{s}(1 - \chi f_t)}, \qquad (45)$$

where $\tilde{J}_{n,t}^H \equiv J_{n,t}^H/\mu_t$ is the employment surplus and μ_t is the multiplier on the budget constraint.

The firm's problem is unchanged, but the Nash bargaining problem maximizes $(\tilde{J}_{n,t})^\eta(\lambda_{n,t})^{1-\eta}$, which implies $\tilde{J}_{n,t} = \eta\lambda_{n,t}/(1 - \eta)$. After combining with (12) and (44), the wage rate is given by

$$w_t = \eta((1 - \alpha)y_y/n_t + \kappa(1 - \chi\bar{s})E_t[x_{t+1}\theta_{t+1}]) + (1 - \eta)\left(b - \frac{(1 - \chi\bar{s})h(z_t)}{1 - f_t - \bar{s}(1 - \chi f_t)}\right), \qquad (46)$$

which replaces (15). Finally, the aggregate resource constraint becomes $c_t + i_t + \kappa v_t + h(z_t)u_t^s = y_t$.

41

Moment	Baseline	Search Effort
$SD(\mathcal{U})$	6.06	5.94
$SD(\tilde{y})$	3.65	3.77
$SD(\tilde{u})$	21.14	24.14
$Corr(\mathcal{U}, \tilde{y})$	-0.62	-0.59

Table 14: Key Moments

Contribution	Output	Uncertainty
Level Total	100.00	39.23
Volatility Total	0.19	61.01
Level Direct	99.81	38.99
Volatility Direct	0.00	60.77

Table 15: Search effort variance decomposition

We assume $h(z_t) = \zeta_0 + \zeta_1 z_t + \zeta_2 z_t^2/2$, where ζ_0 and ζ_1 are set so steady-state search intensity, $\bar{z} = 1$ and there are no search costs in steady state ($h(\bar{z}) = 0$). We set ζ_2 to match the standard deviation of detrended search intensity (2.15), where the time series is constructed by following the approach in Leduc and Liu (2020). This implies $\zeta_2 = 4$, given the parameter estimates in Table 2.

Table 14 compares moments from this model to the baseline model and Table 15 shows the variance decomposition. The model continues to generate a strong negative correlation between output and uncertainty and similar business cycle moments. Level shocks continue to explain almost all of the output variance and about 40% of the uncertainty variance. Therefore, the countercyclical fluctuations in uncertainty remain endogenous and volatility shocks continue to have small real effects.

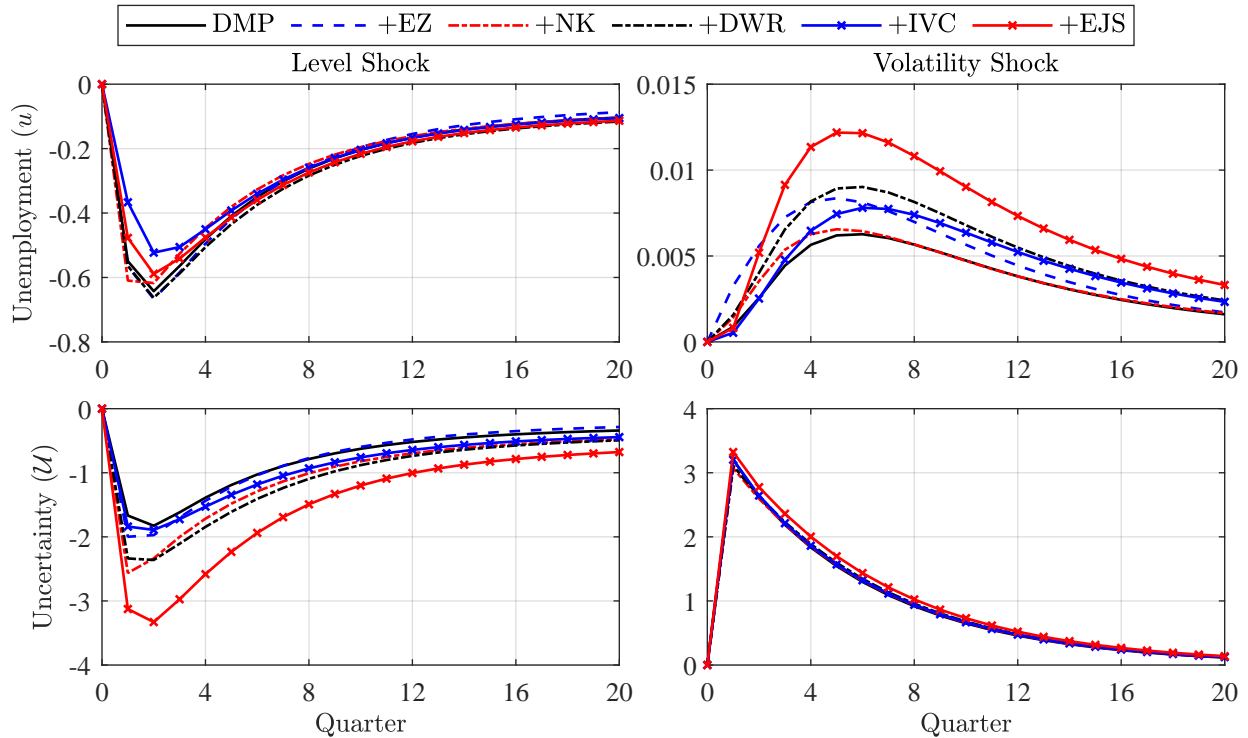## K IMPULSE RESPONSES: EXTENDED DMP MODELS

Figure 5: Generalized impulse responses to 2 standard deviation shocks in the extended DMP models.

L ENDOGENOUS JOB SEPARATIONS MODEL

The following summarizes the equilibrium system for the model with endogenous job separations:

$$v_t = \max\{0, \mu_t\}^2$$

$$\lambda_{v,t} = \max\{0, -\mu_t\}^2$$

$$n_t = (1 - F(\underline{z}_t))((1 - \bar{s})n_{t-1} + m_t)$$

$$u_t = 1 - n_t$$

$$u_t^s = u_{t-1} + \chi\bar{s}n_{t-1}$$

$$\theta_t = v_t/u_t^s$$

$$\mathcal{M}_t = \xi(u_t^s)^\phi v_t^{1-\phi}$$

$$m_t = \min\{\mathcal{M}_t, u_t^s, v_t\}$$

$$q_t = m_t/v_t$$

$$w_t(z_t) = \eta(w_{f,t}z_t + \kappa(1 - \chi\bar{s})E_t[x_{t+1}\theta_{t+1}]) + (1 - \eta)b$$

$$\lambda_{n,t} = \int_{\underline{z}_t}^\infty (w_{f,t}z_t - w_t(z_t))dF(z_t) + (1 - F(\underline{z}_t))(1 - \bar{s})E_t[x_{t+1}\lambda_{n,t+1}]$$

$$w_{f,t}\underline{z}_t - w_t(\underline{z}_t) + (1 - \bar{s})E_t[x_{t+1}\lambda_{n,t+1}] = 0$$

$$q_t\lambda_{n,t} = \kappa - \lambda_{v,t}$$

$$\ell_t = ((1 - \bar{s})n_{t-1} + m_t) \int_{\underline{z}_t}^\infty z_t dF(z_t)$$

$$y_t = a_t k_{t-1}^\alpha \ell_t^{1-\alpha}$$

$$c_t + i_t + \kappa v_t = y_t$$

$$\frac{1}{a_2}\left(\frac{i_t}{k_{t-1}}\right)^{1/\psi} = E_t\left[x_{t+1}\left(r_{t+1}^k + \frac{1}{a_2}\left(\frac{i_{t+1}}{k_t}\right)^{1/\psi}(1 - \delta + a_1) + \frac{1}{\psi-1}\frac{i_{t+1}}{k_t}\right)\right]$$

$$k_t = (1 - \delta)k_{t-1} + \left(a_1 + \frac{a_2}{1-1/\psi}\left(\frac{i_t}{k_{t-1}}\right)^{1-1/\psi}\right)k_{t-1}$$

$$r_t^k = \alpha y_t/k_{t-1}$$

$$w_{f,t} = (1 - \alpha)y_t/\ell_t$$

$$\ln a_t = (1 - \rho_a)\ln\bar{a} + \rho_a \ln a_{t-1} + \sigma_{a,t}\varepsilon_{a,t}$$

$$\ln \sigma_{a,t} = (1 - \rho_{sv})\ln\bar{\sigma}_a + \rho_{sv} \ln \sigma_{a,t-1} + \sigma_{sv}\varepsilon_{sv,t}$$

When $\underline{z} \to 0$, $F(\underline{z}_t) = 0$ and $\int_{\underline{z}_t}^\infty z_t dF(z_t) = 1$, so the model collapses to our baseline DMP model.